Three-body scattering theory without knowledge of exact asymptotic boundary conditions

Robin Shakeshaft*
Department of Physics, University of Southern California, Los Angeles, California 90089-0484, USA
(Received 24 September 2008; published 21 July 2009)

We formulate the theory of three-body scattering without explicit reference to exact asymptotic boundary conditions on the wave function. The transition rate and amplitude are expressed as volume integrals of the resolvent, which are insensitive to the region of asymptotically large distances. The physical branch of the resolvent is selected through the arrow of time, which is required to point forward in each subchannel. This is accomplished by first expressing the resolvent as an integral over time and then making a conformal transformation of each half of the time plane onto a unit disk. The physical branch corresponds to a path of integration in the upper half of the disk. We have tested the method, using a real discrete basis, by calculating the total cross section for singlet *S*-wave electron impact ionization of atomic hydrogen; our results are in reasonable agreement overall with the landmark results of Bartlet and Stelbovics [Phys. Rev. Lett. **93**, 233201 (2004)].

DOI: 10.1103/PhysRevA.80.012708 PACS number(s): 03.65.Nk

I. INTRODUCTION

The three-body scattering problem stands as a bridge between the exactly solvable two-body problem and the complex few- to many-body problem. A deeper understanding of three-body Coulomb scattering is likely to provide further valuable insight into many-body dynamics, a subject of importance in many branches of science and technology. However, the theoretical nonperturbative treatment of three-body atomic scattering remains a significant challenge despite the impressive progress that has been made using current state-of-the-art *ab initio* methods, which include, to cite just a few examples, *R* matrix [1,2], semiclassical *R* matrix [3], *J* matrix [4], pseudostate close coupling [5], convergent close coupling [6], complex exterior scaling [7,8], propagating complex exterior scaling [9,10], Fadeev methods [11,12], spline methods [13], and various approaches based on the numerical integration of the time-dependent Schrödinger equation [14–18]. It is the breakup of the system that poses the most formidable problem. The exact asymptotic form of the wave function for three charged particles at large separations [19] defies an exact numerical description, yet it plays a role, if only formally, in the construction of the amplitude or rate for breakup. Thus the typical calculation of the three-body breakup amplitude or rate calls for the numerical integration of the (time-dependent or time-independent) Schrödinger equation to very large distances.

In this paper we formulate the theory of a stationary three-body scattering process without explicitly addressing asymptotic boundary conditions. Assuming that two of the bodies are initially bound to one another, we derive various expressions for the asymptotic flux, and hence the transition rate, in terms of volume integrals. These expressions are insensitive to the region of asymptotically large distances since the dominant contribution comes from the interaction region, a region that can be covered by a finite discrete basis. We focus on the resolvent rather than the wave function. The advantage of doing so is that the resolvent is independent of the asymptotic configuration of the system. Indeed, it is subject to a unique constraint, which is that among its many branches only *one*—the "physical" branch—is acceptable. In contrast, many possible (sub)channels are available to a few-body system, and, accordingly, the asymptotic boundary condition on the wave function is not unique.

The physical branch of the resolvent can be specified, at least formally, by the requirement that the scattered wave in *each* (sub)channel is an *out*going complex wave. In practice this requirement may not be straightforward to implement. If the wave function of the system is represented on a *real* discrete basis, as is commonly done, outgoing waves cannot be distinguished from ingoing waves. If a *complex* discrete basis (one whose basis functions have a complex length scale) is employed, as is also commonly done, outgoing *or* ingoing waves, but *not both*, can be mimicked. This does not pose a limitation if the process of interest is a half-collision one, e.g., the photodecay of an atomic system, since only outgoing waves are present, and a complex basis can be employed to readily calculate rates for partial and total decay without knowledge of the exact asymptotic form of the wave function [20,21]. However, a conventional collision involves both incoming and outgoing waves. Furthermore, since the asymptotic boundary conditions appropriate to a conventional scattering process are *real* standing-wave boundary conditions, the natural basis on which to represent the wave function is a real one. Besides, a real basis demands half the storage and execution time of a complex basis. More importantly, while complex basis functions are analytic in the length scale, the complex-conjugate basis functions are not analytic in this length scale and as a consequence expressions constructed from both the wave function and its complex conjugate do not have predictable convergence with respect to increasing basis size.

An alternative way to specify the physical branch is through the time rather than the spatial coordinates of the system. In our world, time's arrow points forward, yet time-reversal invariance permits a microscopic system to evolve forward or backward. The physical branch is the one for which time's arrow points forward in *each* (sub)channel. The nonphysical branches are those for which time's arrow points backward in some, perhaps all, (sub)channels. In place of

*robins@usc.edu

many spatial coordinates we specify the physical branch through a single time coordinate. At first sight the reintroduction of the time into the description of a *stationary* process might seem like a needless increase in the number of dimensions but it allows us to fully exploit the symmetry of time-reversal invariance [22].

The resolvent $G(E) \equiv 1/(E-H)$ for a system whose Hamiltonian and energy are H and E, respectively, has an underlying time scale, t_0, say, which we expose by writing

$$G(E) = -it_0 \int_0^\infty d\tau e^{i(t_0 E)\tau} U(t_0 \tau), \tag{1}$$

where $\tau = t/t_0$ is a dimensionless time and where $U(t)$ is the time-translation operator:

$$U(t) = e^{-itH}. \tag{2}$$

We have chosen units in which $\hbar = 1$. We are free to shift the eigenvalue spectrum of H by any amount, as long as we shift E by the same amount, thereby leaving $E-H$ unchanged. For a reason explained below, it is useful to shift the spectrum so that H is *positive definite*. Thus we include in H an amount Δ that is slightly larger than the ground-state binding energy of the three-body system. Furthermore, since we are interested in describing a scattering process we suppose that E lies in the continuous spectrum of H; i.e., we restrict E to the range $E > \Delta_0 > 0$ where Δ_0 is the lowest (shifted) threshold for partial breakup of the three-body system. The spectrum of H is effectively bounded from above since the asymptotically large-energy components of any physically reasonable wave packet on which $G(E)$ may act play no significant role. Thus it takes a finite (not infinitesimal) time for a wave packet to evolve noticeably under the influence of H; it is this time which is characterized by t_0. For definiteness we assign to t_0 the value

$$t_0 = \frac{1}{E + \Delta - \Delta_0}, \tag{3}$$

a time scale that incorporates both the times $1/(E-\Delta_0)$ and $1/\Delta$, which characterize the duration and strength, respectively, of the interactions. Note that $Et_0 < 1$ since $\Delta_0 < \Delta$; typically $Et_0 \sim 1$.

The dichotomy posed by time's arrow is illustrated by the correlation amplitude $C(t) \equiv \langle a|U(t)|a\rangle$, where $|a\rangle$ is a normalizable ket that represents a physically realistic, spatially localized, wave packet at time $t=0$. Let us decompose $|a\rangle$ into the two orthogonal components $|a_{\rm bd}\rangle$ and $|a_{\rm ct}\rangle$, which lie, respectively, in the subspaces spanned by the bound- and continuum-state eigenkets of H. We have $C(t) = C_{\rm bd}(t) + C_{\rm ct}(t)$ where $C_{\rm bd}(t) = \langle a_{\rm bd}|U(t)|a_{\rm bd}\rangle$ and $C_{\rm ct}(t) = \langle a_{\rm ct}|U(t)|a_{\rm ct}\rangle$. As the wave packet evolves the continuum-state component $U(t)|a_{\rm ct}\rangle$ diffuses throughout space and becomes completely unlocalized in the limit $t \to \infty$, while the bound-state component $U(t)|a_{\rm bd}\rangle$ remains localized, periodically returning to (or almost to) its original form $|a_{\rm bd}\rangle$ up to an overall phase factor. An informal examination [23] of $C(t)$ reveals that $C_{\rm ct}(t)$ has a pair of second-order branch points, one at $t=\infty$ and the other on the positive imaginary axis at a distance of the order of t_0 from the origin. In contrast, $C_{\rm bd}(t)$ is free of branch-point singularities but it has an essential singularity at $t=\infty$. The branch point at $t \sim it_0$ sets the time scale of the system's evolution while the branch point at $t=\infty$ signifies that the state reached by an unlocalized system is double valued; for although the system can be prepared in a unique state at any finite time, say $t=0$, it can evolve either forward or backward and the state at the single point $t=\infty$ depends on the direction of evolution to this point. The essential singularity at $t=\infty$ signifies that the state reached by a localized system oscillates without limit and is undefined at $t=\infty$. Since a three-body system can have two-body bound states, $C_{\rm ct}(t)$ also has an essential singularity at $t=\infty$.

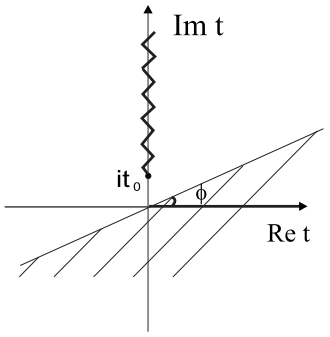

FIG. 1. The temporal correlation amplitude has a branch point on the positive imaginary time axis that is paired with another one at infinity. The correlation amplitude is free of singularities in any finite region of the complex time plane below the line Im t/Re t = tan ϕ; this region can be conformally mapped onto a unit disk.

The path of integration on the right side of Eq. (1) is along the positive real τ axis; this path yields the physical branch of the resolvent. Were we to choose a path along the negative real τ axis, we would obtain the unphysical branch corresponding to time's arrow pointing backward in all subchannels. We could (we do not) rotate the path of integration into the upper right quadrant of the complex τ plane, but we would have to first project out the closed subchannels [24] since they give rise to an essential singularity at $\tau=\infty$ (the essential singularity arising from the open subchannels is damped out by the factor e^{iEt}).

Since time is a parameter, not a dynamical variable, the properties that $G(E)$ has with respect to its underlying time are not specific to the Hamiltonian. Therefore the method we develop below is very general. It does not depend on the nature of H, aside from the requirement that H be invariant under time reversal, nor does it depend on the way in which H is represented. It is equally applicable to half- and full-collisions when a real basis is employed. As a test, we applied it to singlet S-wave electron impact ionization of atomic hydrogen, and we obtained results for the total ionization cross section that are in reasonable agreement, overall, with the benchmark results of Bartlett and Stelbovics [9].

We can eliminate, or rather render innocuous, the branch point at $\tau \sim i$ by making a conformal transformation that maps one half of the complex τ plane onto the unit disk $|u| < 1$ and the other half onto the region $|u| > 1$ outside the disk. Thus we divide the τ plane into two half-planes by the boundary Im τ/Re τ=tan ϕ, where $0 < \phi < \pi/2$; see Fig. 1. The mapping is

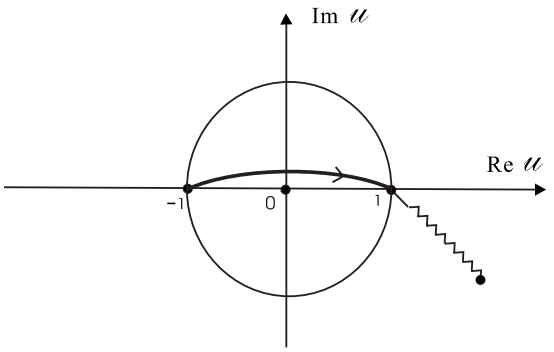

FIG. 2. One half of the τ plane is mapped onto the unit disk $|u|<1$. The physical branch of the resolvent is associated with an integration contour in the τ plane, which runs from 0 to ∞ along the positive real τ axis or more generally along a ray in the sector $0\leq \arg(\tau)\leq \phi$. This contour is mapped onto a path in the u plane, which runs from $u=-1$ to $u=1$ in the upper half of the unit disk. The branch cut (zigzag line) lies outside the disk.

$$u=\frac{\tau+ie^{i\phi}}{\tau-ie^{i\phi}}, \tag{4}$$

and its inverse is

$$\tau=-ie^{i\phi}\left(\frac{1+u}{1-u}\right). \tag{5}$$

Note, incidentally, that $\tau\to-\tau$ implies $u\to 1/u$. The transformation from τ to u places the finite branch point outside the disk. The contour of integration on the right side of Eq. (1), i.e., the line along the real positive τ axis, or more generally a ray in the sector $0\leq\arg(\tau)\leq\phi$, is transformed to a path from $u=-1$ to $u=1$ in the *upper* half of the disk; see Fig. 2. If we were to seek the unphysical branch we would choose ϕ to be in the range $-\pi/2<\phi<0$; the line along the real negative τ axis, or more generally a ray in the sector $\pi+\phi\leq\arg(\tau)\leq\pi$, would be transformed to a path from $u=-1$ to $u=1$ in the *lower* half of the disk. Thus a contour in the upper (lower) half of the unit disk in the u plane is associated with the physical (an unphysical) branch. Once we have fixed the branch to be the physical one we can extend the range of ϕ to $0<\phi<\pi$. The "physical" energy sheet is $-\phi<\arg(E)<2\pi-\phi$. A resonance pole, at $E_{\rm res}$ say, lies on the physical sheet if $\phi>\arg(E_{\rm res})$.

The time-translation operator can be expanded in powers of u by making use of the generating function for the associated Laguerre polynomials $L_n^{(m)}(2z)$, i.e.,

$$\frac{1}{(1-u)^{m+1}}\exp\left(\frac{2zu}{u-1}\right)=\sum_{n=0}^{\infty}L_n^{(m)}(2z)u^n. \tag{6}$$

Setting $m=1$ the left side of Eq. (6) is a perfect derivative with respect to u:

$$\frac{d}{du}\exp\left(\frac{2zu}{u-1}\right)=-2z\sum_{n=0}^{\infty}L_n^{(1)}(2z)u^n. \tag{7}$$

Integrating over u from 0 to an indefinite upper limit gives

$$\exp\left(\frac{2zu}{u-1}\right)=1-2z\sum_{n=1}^{\infty}\frac{1}{n}L_{n-1}^{(1)}(2z)u^n, \tag{8}$$

and putting $z=t_\phi H$, where t_ϕ is a complex unit of time defined as

$$t_\phi\equiv t_0e^{i\phi}, \tag{9}$$

we arrive at

$$U(t)=e^{-t_\phi H}\left[1-2t_\phi H\sum_{n=1}^{\infty}\frac{1}{n}L_{n-1}^{(1)}(2t_\phi H)u^n\right]. \tag{10}$$

This series converges for all $|u|<1$. The prefactor $e^{-t_\phi H}$ appropriately diminishes the role of eigenvalues of H that are much larger than $1/t_0$ (noting that typically $\phi\ll\pi/2$).

At this stage we can explain why we have chosen H to be positive definite: at $u=1$, where t is infinite, there is both a branch point and an essential singularity. The rate of convergence of the power-series representation of $U(t)$ for u inside the unit disk but close to the essential singularity depends on the behavior of $U(t)$ at large t, which in turn depends on the sector of the t plane in which t lies. We allow t to approach infinity along our contour of integration and (assuming that we exclude the closed subchannels) this contour can lie within and on the boundaries of the sector $0<\arg(t)<\phi$. Suppose that $U(t)$ acts on an eigenket of H with an eigenvalue $\mathcal{E}$, and that t approaches infinity within the allowed sector, $U(t)$ increases or decreases exponentially according to whether $\mathcal{E}$ is positive or negative, respectively. Now, the relative error incurred from truncating a power-series expansion of an exponential function is much smaller if the function is an exponentially growing one than if it is an exponentially decreasing one. Consequently, we shift the spectrum of H to ensure that it has no negative eigenvalues.

We turn now to the branch point at $u=1$. We have already selected the physical branch of the resolvent through our choice of the phase of the unit of time t_ϕ, which ensures that the contour of integration lies in the upper half of the unit disk. Therefore the branch point at the end of the contour is more of a technical nuisance than a feature that carries physical consequences. Indeed, in practice H must be represented by a finite-dimensional matrix, so the maximum time interval over which the evolution of the system can be described adequately is characterized by the dimensionless time [25]

$$\mathcal{T}_{\rm max}=1/(t_0\Delta E), \tag{11}$$

where ΔE is the (positive) separation of the two eigenvalues adjacent to E. (We assume that the eigenvalue spectrum is sufficiently dense in the neighborhood of E that $\mathcal{T}_{\rm max}\gg 1$.) Therefore it is consistent with practice to replace the upper infinite limit on the time integral by a finite number $\mathcal{T}$ of order $\mathcal{T}_{\rm max}$; thus Eq. (1) becomes

$$\frac{1-e^{it_0E\mathcal{T}}U(t_0\mathcal{T})}{E-H}=-it_0\int_0^{\mathcal{T}}d\tau\, e^{it_0E\tau}U(t_0\tau). \tag{12}$$

The regions $\tau\ll\mathcal{T}_{\rm max}$ and $\tau\sim\mathcal{T}_{\rm max}$, respectively, contribute to the off-shell (principal value) and on-shell (energy-

conserving) parts of $G(E)$. Substituting the right side of Eq. (10) for $U(t_0\tau)$ in Eq. (12) and integrating over τ gives

$$\frac{1-e^{it_0ET}U(t_0\mathcal{T})}{E-H} = -it_\phi e^{-t_\phi H}\left[\mathcal{I}_0(2Et_\phi,\mathcal{T}_{-\phi}) - 2t_\phi H\sum_{n=1}^{\infty}\frac{1}{n}\mathcal{I}_n(2Et_\phi,\mathcal{T}_{-\phi})L_{n-1}^{(1)}(2t_\phi H)\right], \tag{13}$$

where

$$\mathcal{T}_\phi = \mathcal{T}e^{i\phi} \tag{14}$$

and where the coefficient $\mathcal{I}_n(2z,w)$, which is a function of the two variables $z=Et_\phi$ and $w=\mathcal{T}_{-\phi}$, is defined as the integral

$$\mathcal{I}_n(2z,w) = e^{-i\phi}\int_0^{\mathcal{T}} d\tau\, e^{i(ze^{-i\phi})\tau}u^n \tag{15}$$

$$= w\int_0^1 ds\, e^{i(zw)s}\left(\frac{sw+i}{sw-i}\right)^n, \tag{16}$$

where $s=\tau/\mathcal{T}$. The integrals $\mathcal{I}_n(2z,w)$ can be evaluated efficiently by means of a recurrence relation developed in Sec. III. The on-shell part of the series on the right side of Eq. (13) converges after roughly $(Et_0)\mathcal{T}^2$ terms are included.

Since we have moved the branch point at $t\sim it_0$ outside the unit disk, the off-shell part of $G(E)$ is stable as $\mathcal{T}$ increases, but the on-shell part fluctuates due to the proximity of the branch point at $t=\infty$. However, we can obtain a definite limit either by Padé extrapolation of a sequence of terms, each evaluated at different, equally spaced values of $\mathcal{T}$, or by smoothing out the fluctuations through temporal averaging. When $U(t_0\mathcal{T})$ acts on a superposition of bound-state eigenkets of H, the superposition oscillates out of phase with e^{it_0ET}, and without limit, as $\mathcal{T}$ increases, so the combination $e^{it_0ET}U(t_0\mathcal{T})$ vanishes if it is averaged over a long time interval of order $\mathcal{T}_{\max}$. When $U(t_0\mathcal{T})$ acts on a normalizable ket, which is orthogonal to the bound-state eigenkets of H, it decreases along each spatial coordinate as $1/\mathcal{T}^{1/2}$ due to wave packet spreading. Therefore if $|a\rangle$ and $|b\rangle$ are any two normalizable kets, which may contain bound-state components, the large-$\mathcal{T}$ average of $\langle b|e^{it_0ET}U(t_0\mathcal{T})|a\rangle$ vanishes.

It follows that if we average both sides of Eq. (13) over large values of the upper limit $\mathcal{T}\sim\mathcal{T}_{\max}$, the term $e^{it_0ET}U(t_0\mathcal{T})$ disappears and the left side averages to the resolvent $G(E)$. Only the on-shell contribution to the resolvent is sensitive to averaging—the off-shell contribution is independent of $\mathcal{T}$ if $\mathcal{T}\gg 1$. We find that temporal averaging yields meaningful and fairly stable matrix elements of the resolvent and is an alternative (not necessarily a better one) to *spatial* averaging, which was used long ago [26,27] and has been advocated again more recently [28] to deal with formally divergent integrals that appear in variational identities for three-body scattering. Padé extrapolation, which effects an implicit average over time, is even more robust and will be taken up elsewhere.

In the next section we derive various expressions for the transition rate in terms of volume integrals of the resolvent. In Sec. III we discuss the evaluation of the sum over n and its coefficients $\mathcal{I}_n(2z,\mathcal{T}_{-\phi})$, which appear in Eq. (13). In Sec. IV we discuss the error incurred by truncating the expansion of $U(t)$ in powers of u on the right side of Eq. (10). Since the power-series representation of $U(t)$ does not converge on the edge $|u|=1$ of the disk, it does not converge at either end point of the contour of integration in the u plane. Therefore, it fails to give the correct result $U(0)=1$ even though there is no singularity at $u=-1$. Nevertheless, we see in Sec. IV that we can reproduce the result $U(0)=1$ if we truncate the power series after a large number of terms and average over this number. In Sec. V we discuss variational principles for both $U(t)$ and $G(E)$. In Sec. VI we describe and present results of our test application to singlet S-wave electron impact ionization of atomic hydrogen. In Appendix A we compare the sum over n on the right side of Eq. (13) with an analogous expansion of the resolvent in Chebyshev polynomials developed by Mandelshtam and Taylor [29]. In contrast to Eq. (13), which is based on the temporal development of the system, the Chebyshev expansion is based on the spatial development. In Appendix B we study several different sums of Laguerre polynomials that arise in the formulation of our approach. In Appendix C we describe a method for treating potential scattering that is suitable when an analytic basis is employed; this method is used to account for the distortion of the incident plane wave in our application to electron impact ionization of atomic hydrogen.

II. FLUX FORMULAS

We consider a system that consists of three structureless particles, two of which are initially bound to one another. Let H_{in} be the channel Hamiltonian for the in-channel (the entrance channel); the perturbation in this channel is

$$W_{\text{in}} \equiv H - H_{\text{in}}. \tag{17}$$

Let $|\psi_{\text{in}}\rangle$ represent the initial unperturbed state of the system. We have

$$H_{\text{in}}|\psi_{\text{in}}\rangle = E|\psi_{\text{in}}\rangle. \tag{18}$$

It is useful to attach a superscript to the resolvent to distinguish it from its adjoint; the physical resolvent is $G^+(E)=1/(E-H)$ while $G^-(E)=[G^+(E)]^\dagger$, where here E is understood to be real.

A. Inclusive transition rate

The *inc*lusive rate Γ_{inc} for transitions to all energetically accessible states is proportional to the net asymptotic flux, i.e.,

$$\Gamma_{\text{inc}} = i\langle\psi_{\text{in}}|[G^+(E)W_{\text{in}}]^\dagger(H-H^\dagger)G^+(E)W_{\text{in}}|\psi_{\text{in}}\rangle. \tag{19}$$

Using Green's theorem the matrix element on the right side of Eq. (19) can be rewritten as a surface integral over the surface at infinity; for computational purposes, however, it is more useful to express this matrix element as a volume integral (whose integrand vanishes at infinity):

$$\Gamma_{\text{inc}} = i\langle\psi_{\text{in}}|[G^+(E)W_{\text{in}}]^\dagger[(E-H)^\dagger - (E-H)]G^+(E)W_{\text{in}}|\psi_{\text{in}}\rangle \tag{20}$$

$$= -2\ \text{Im}\langle\psi_{\text{in}}|[(E-H)G^+(E)W_{\text{in}}]^\dagger G^+(E)W_{\text{in}}|\psi_{\text{in}}\rangle \tag{21}$$

$$= -2\ \text{Im}\langle\psi_{\text{in}}|W_{\text{in}}G^+(E)W_{\text{in}}|\psi_{\text{in}}\rangle. \tag{22}$$

To facilitate comparison with expressions that are developed below it is instructive to rewrite Eq. (22) in a more familiar form, in terms of the eigenket of H, say $|\Psi_{\text{in}}^{\pm}\rangle$, which represents the state that evolves forward from (+) or backward to (−) the initial state. Since

$$|\Psi_{\text{in}}^{\pm}\rangle = |\psi_{\text{in}}\rangle + G^{\pm}(E)W_{\text{in}}|\psi_{\text{in}}\rangle, \tag{23}$$

we have, noting that $W_{\text{in}}G^+(E)=[G^-(E)W_{\text{in}}]^\dagger$, and observing that since W_{in} is Hermitian $\langle\psi_{\text{in}}|W_{\text{in}}|\psi_{\text{in}}\rangle$ is real and therefore does not contribute to Γ_{inc},

$$\Gamma_{\text{inc}} = -2\ \text{Im}\langle\psi_{\text{in}}|W_{\text{in}}|\Psi_{\text{in}}^+\rangle \tag{24}$$

$$= -2\ \text{Im}\langle\Psi_{\text{in}}^-|W_{\text{in}}|\psi_{\text{in}}\rangle. \tag{25}$$

Equations (24) and (25) are the usual statements of the optical theorem for scattering.

B. Partial transition rate

The optical theorem does not give detailed information about the scattering process, but the steps that we took to this theorem also lead the way toward the partial rate for transitions to a particular group of energetically accessible states. Let P denote a projection operator, which projects onto the in-channel or onto a group of subchannels within the in-channel that includes the initial state, so that

$$P|\psi_{\text{in}}\rangle = |\psi_{\text{in}}\rangle. \tag{26}$$

We denote the complement of P by $Q \equiv 1-P$. We have

$$Q|\psi_{\text{in}}\rangle = 0. \tag{27}$$

It is convenient to isolate that part of H, say H_0, which commutes with P and therefore with Q:

$$H \equiv H_0 + W_0, \tag{28}$$

$$[P,H_0] = 0, \tag{29}$$

where the interaction W_0 vanishes for asymptotically large separations of the particles. Let Γ_Q denote the rate for transitions to those states that lie in Q space. Since the right side of Eq. (19) can be expressed as a surface integral, its value is determined entirely by the asymptotic behavior of $G^+(E)W_{\text{in}}|\psi_{\text{in}}\rangle$ in position space. To extract Γ_Q we need only let Q project onto $G^+(E)W_{\text{in}}|\psi_{\text{in}}\rangle$ at the surface; we have

$$\Gamma_Q = i\langle\psi_{\text{in}}|[G^+(E)W_{\text{in}}]^\dagger Q(H-H^\dagger)QG^+(E)W_{\text{in}}|\psi_{\text{in}}\rangle. \tag{30}$$

Noting that $H-H^\dagger = H_0 - H_0^\dagger$, that Q commutes with H_0, and that $Q^2=Q$, we can re-express Γ_Q as

$$\Gamma_Q = i\langle\psi_{\text{in}}|[G^+(E)W_{\text{in}}]^\dagger Q[(E-H_0)^\dagger - (E-H_0)]QG^+(E)W_{\text{in}}|\psi_{\text{in}}\rangle \tag{31}$$

$$= -2\ \text{Im}\langle\psi_{\text{in}}|[(E-H_0)G^+(E)W_{\text{in}}]^\dagger QG^+(E)W_{\text{in}}|\psi_{\text{in}}\rangle \tag{32}$$

$$= -2\ \text{Im}\{\langle\psi_{\text{in}}|W_{\text{in}}QG^+(E)W_{\text{in}}|\psi_{\text{in}}\rangle + \langle\psi_{\text{in}}| \times [W_0G^+(E)W_{\text{in}}]^\dagger QG^+(E)W_{\text{in}}|\psi_{\text{in}}\rangle\} \tag{33}$$

$$= -2\ \text{Im}\{\langle\psi_{\text{in}}|W_{\text{in}}QG^+(E)W_{\text{in}}|\psi_{\text{in}}\rangle + \langle\psi_{\text{in}}|W_{\text{in}}G^-(E)W_0QG^+(E)W_{\text{in}}|\psi_{\text{in}}\rangle\} \tag{34}$$

$$= -2\ \text{Im}\langle\psi_{\text{in}}|(W_{\text{in}}-W_0)QG^+(E)W_{\text{in}}|\psi_{\text{in}}\rangle - 2\ \text{Im}\langle\psi_{\text{in}}|[1+W_{\text{in}}G^-(E)]W_0QG^+(E)W_{\text{in}}|\psi_{\text{in}}\rangle, \tag{35}$$

where in the last line we subtracted and added the same term in order to facilitate the following simplification: noting that $W_{\text{in}}-W_0=H_0-H_{\text{in}}$ we have

$$\langle\psi_{\text{in}}|(W_{\text{in}}-W_0)Q = \langle\psi_{\text{in}}|(H_0-H_{\text{in}})Q. \tag{36}$$

Since Q and H_0 commute we can move Q to the left of H_0 on the right side of Eq. (36). Furthermore, since $\langle\psi_{\text{in}}|$ is an eigenbra of H_{in} we can move Q to the left of H_{in}. Recalling Eq. (27) it follows that both $\langle\psi_{\text{in}}|H_0Q$ and $\langle\psi_{\text{in}}|H_{\text{in}}Q$ are null kets. Hence the first term on the right side of Eq. (35) vanishes. Recalling that $\langle\psi_{\text{in}}|P=\langle\psi_{\text{in}}|$, writing $W_0Q=PW_0Q+QW_0Q$, and noting that since QW_0Q is Hermitian it does not contribute to Γ_Q, it follows that

$$\Gamma_Q = -2\ \text{Im}\langle\psi_{\text{in}}|[1+W_{\text{in}}G^-(E)]PW_0QG^+(E)W_{\text{in}}|\psi_{\text{in}}\rangle \tag{37}$$

$$= -2\ \text{Im}\langle\Psi_{\text{in}}^+|PW_0QG^+(E)W_{\text{in}}|\psi_{\text{in}}\rangle \tag{38}$$

$$= -2\ \text{Im}\langle\Psi_{\text{in}}^+|PW_0Q|\Psi_{\text{in}}^+\rangle, \tag{39}$$

where we used Eqs. (23) and (27) in the last step. Comparing Eq. (39) for the partial rate with Eq. (24) for the inclusive rate we see that in place of the perturbation W_{in} we now have PW_0Q; in addition, the partial rate is bilinear rather than linear in $|\Psi_{\text{in}}^+\rangle$. We cannot recover Eq. (24) by putting $Q=1$ in Eq. (39) since we have used Eqs. (26) and (27). Taking the complex conjugate of Eq. (39) gives the alternative expression

$$\Gamma_Q = 2\ \text{Im}\langle\Psi_{\text{in}}^+|QW_0P|\Psi_{\text{in}}^+\rangle. \tag{40}$$

We can obtain the rate for transitions to a subspace of Q space by replacing Q, in the preceding expressions, by the operator which projects onto that subspace. Note that while Eq. (40) has the virtue of compactness, Eq. (37) displays the resolvent explicitly and is therefore more convenient for computational purposes.

Now we derive the partial rate, Γ_P, for transitions to P space, and in doing so we confirm the law of conservation of flux. Repeating the steps that led from Eq. (30) to Eq. (35), this time with Q replaced by P, we obtain

$$\Gamma_P = -2\,\mathrm{Im}\langle\psi_{\mathrm{in}}|(W_{\mathrm{in}} - W_0)PG^+(E)W_{\mathrm{in}}|\psi_{\mathrm{in}}\rangle - 2\,\mathrm{Im}\langle\psi_{\mathrm{in}}|[1 + W_{\mathrm{in}}G^-(E)]W_0PG^+(E)W_{\mathrm{in}}|\psi_{\mathrm{in}}\rangle, \tag{41}$$

Using Eq. (36), now with P in place of Q, we can use the same argument as above to move P to the left of $(W_{\mathrm{in}} - W_0)$ in the first term on the right side of Eq. (41), whereupon it can be replaced by the identity. Therefore, noting that $\langle\psi_{\mathrm{in}}|(W_{\mathrm{in}} - W_0)P|\psi_{\mathrm{in}}\rangle$ is real, the first term on the right side of Eq. (41) is the same as $-2\,\mathrm{Im}\langle\psi_{\mathrm{in}}|(W_{\mathrm{in}} - W_0)|\Psi_{\mathrm{in}}^+\rangle$. The second term is

$$-2\,\mathrm{Im}\langle\Psi_{\mathrm{in}}^+|W_0PG^+(E)W_{\mathrm{in}}|\psi_{\mathrm{in}}\rangle = -2\,\mathrm{Im}\langle\Psi_{\mathrm{in}}^+|W_0P|\Psi_{\mathrm{in}}^+\rangle + 2\,\mathrm{Im}\langle\Psi_{\mathrm{in}}^+|W_0|\psi_{\mathrm{in}}\rangle. \tag{42}$$

It follows that

$$\Gamma_P = -2\,\mathrm{Im}\langle\psi_{\mathrm{in}}|W_{\mathrm{in}}|\Psi_{\mathrm{in}}^+\rangle - 2\,\mathrm{Im}\langle\Psi_{\mathrm{in}}^+|QW_0P|\Psi_{\mathrm{in}}^+\rangle \tag{43}$$

$$= \Gamma_{\mathrm{inc}} - \Gamma_Q, \tag{44}$$

where in the first step we noted that the imaginary parts of $\langle\Psi_{\mathrm{in}}^+|W_0P|\Psi_{\mathrm{in}}^+\rangle$ and $\langle\Psi_{\mathrm{in}}^+|QW_0P|\Psi_{\mathrm{in}}^+\rangle$ are the same, and in the second step we used Eqs. (24) and (40).

C. Distorted-wave formulation

We can incorporate some of the (non-Coulombic) distortion of the initial state by using the distorted-wave formalism. The strategy is to find a potential that reduces the strength of the perturbation in the entrance channel yet is sufficiently simple that the wave function for scattering from this potential can be determined exactly. Here we choose a "static" potential W_{st}, which cannot induce transitions out of P space, i.e.,

$$PW_{\mathrm{st}}Q = 0. \tag{45}$$

For example, we could choose W_{st} to be $PW_{\mathrm{in}}P$. The distorted-wave perturbation in the entrance channel is

$$W_{\mathrm{d}} \equiv W_{\mathrm{in}} - W_{\mathrm{st}}, \tag{46}$$

and the distorted-wave channel Hamiltonian is

$$H_{\mathrm{d}} \equiv H_{\mathrm{in}} + W_{\mathrm{st}}. \tag{47}$$

Introducing

$$G_{\mathrm{d}}(E) \equiv 1/(E - H_{\mathrm{d}}), \tag{48}$$

the distorted initial state is represented by

$$|\psi_{\mathrm{d}}^{\pm}\rangle = |\psi_{\mathrm{in}}\rangle + G_{\mathrm{d}}^{\pm}(E)W_{\mathrm{st}}|\psi_{\mathrm{in}}\rangle. \tag{49}$$

We can rewrite Eq. (23) as [30]

$$|\Psi_{\mathrm{in}}^{\pm}\rangle = |\psi_{\mathrm{d}}^{\pm}\rangle + G^{\pm}(E)W_{\mathrm{d}}|\psi_{\mathrm{d}}^{\pm}\rangle \tag{50}$$

and substitute the right side of Eq. (50) for $|\Psi_{\mathrm{in}}^+\rangle$ into Eq. (40). Since W_{st} does not induce transitions out of P space,

$$Q|\psi_{\mathrm{d}}^{\pm}\rangle = 0, \tag{51}$$

but up to now we have not used this property. If we do use it we can go back to Eq. (37) and replace $|\psi_{\mathrm{in}}\rangle$ and W_{in} by $|\psi_{\mathrm{d}}^+\rangle$ and W_{d}, respectively: to see this we first use Eqs. (23) and (50) to write

$$G^{\pm}(E)W_{\mathrm{in}}|\psi_{\mathrm{in}}\rangle = G^{\pm}(E)W_{\mathrm{d}}|\psi_{\mathrm{d}}^{\pm}\rangle + |\psi_{\mathrm{d}}^{\pm}\rangle - |\psi_{\mathrm{in}}\rangle, \tag{52}$$

$$\langle\psi_{\mathrm{in}}|W_{\mathrm{in}}G^{\pm}(E) = \langle\psi_{\mathrm{d}}^{\mp}|W_{\mathrm{d}}G^{\pm}(E) + \langle\psi_{\mathrm{d}}^{\mp}| - \langle\psi_{\mathrm{in}}|. \tag{53}$$

Now we use Eqs. (52) and (53) to substitute for $G^+(E)W_{\mathrm{in}}|\psi_{\mathrm{in}}\rangle$ and $\langle\psi_{\mathrm{in}}|W_{\mathrm{in}}G^-(E)$ in Eq. (37). We follow by using Eqs. (27) and (51), which yields the desired result:

$$\Gamma_Q = -2\,\mathrm{Im}\langle\psi_{\mathrm{d}}^+|[1 + W_{\mathrm{d}}G^-(E)]PW_0QG^+(E)W_{\mathrm{d}}|\psi_{\mathrm{d}}^+\rangle, \tag{54}$$

$$= 2\,\mathrm{Im}\langle\psi_{\mathrm{d}}^+|W_{\mathrm{d}}G^-(E)QW_0P[1 + G^+(E)W_{\mathrm{d}}]|\psi_{\mathrm{d}}^+\rangle, \tag{55}$$

where the second line is the complex conjugate of the first.

The distorted-wave form of the inclusive rate follows by using Eq. (52) to substitute for $G^+(E)W_{\mathrm{in}}|\psi_{\mathrm{in}}\rangle$ in Eq. (22) and subsequently using Eq. (53) to substitute for $\langle\psi_{\mathrm{in}}|W_{\mathrm{in}}G^+(E)$; after using Eq. (46) we arrive at

$$\Gamma_{\mathrm{inc}} = -2\,\mathrm{Im}\langle\psi_{\mathrm{in}}|W_{\mathrm{st}}|\psi_{\mathrm{d}}^+\rangle - 2\,\mathrm{Im}\langle\psi_{\mathrm{d}}^-|W_{\mathrm{d}}[1 + G^+(E)W_{\mathrm{d}}]|\psi_{\mathrm{d}}^+\rangle. \tag{56}$$

This is a restatement of the optical theorem within the distorted-wave formalism and of course we have not used any properties of Q in deriving it. The first term on the right side of Eq. (56) is the rate for scattering from the static potential alone.

D. Transition amplitude

Finally, we consider the transition amplitude rather than the rate. Evaluation of the amplitude requires more information about the final state than we have needed up to now. Let $|\Psi_{\mathrm{out}}^{\pm}\rangle$ be the eigenket of H, which represents the state that evolves forward to (−) or backward from (+) the final state of interest. The transition amplitude is

$$A = \langle\Psi_{\mathrm{out}}^-|(H^\dagger - H)G^+(E)W_{\mathrm{in}}|\psi_{\mathrm{in}}\rangle. \tag{57}$$

Since the asymptotic boundary condition on the wave function for a bound-continuum channel (in which two of the particles are bound) is well known and relatively simple, we focus on the breakup process. Therefore we choose Q to project onto the breakup channel, i.e., onto the space occupied by three particles at asymptotically large separations. Eigenkets of H that are associated with different channels are orthogonal. Hence the matrix element on the right side of Eq. (57) contains no contribution from scattering to a bound-continuum channel. If this matrix element is converted to a surface integral, the contribution from the surface region where two particles are near to one another, with the third far away, washes out upon integration. This is the region on which P projects, and therefore we can insert $Q = 1 - P$ to the right of $\langle\Psi_{\mathrm{out}}^-|$ without altering the value of the breakup amplitude:

$$A = \langle\Psi_{\mathrm{out}}^-|Q(H^\dagger - H)G^+(E)W_{\mathrm{in}}|\psi_{\mathrm{in}}\rangle. \tag{58}$$

We make this replacement so as not to incur a spurious contribution to the breakup amplitude from scattering within a

bound-continuum channel when we approximate $|\Psi^{\pm}_{\text{out}}\rangle$. Contamination of the continuum-continuum channel by bound-continuum subchannels was highlighted by Bouri *et al.* [3], who took special care to avoid it in their study of double photoionization of helium just above the breakup threshold.

Since the right side of Eq. (58) can be expressed as a surface integral, its value is determined entirely by the asymptotic behavior of $|\Psi^{\pm}_{\text{out}}\rangle$ in position space. With this in mind we decompose the Hamiltonian as

$$H \equiv H_{\text{eff}} + W_{\text{eff}}, \tag{59}$$

where H_{eff} is a simple effective Hamiltonian and we introduce the ansatz $|\Psi^{\pm}_{\text{eff,out}}\rangle$, which is an eigenket of H_{eff}:

$$H_{\text{eff}}|\Psi^{\pm}_{\text{eff,out}}\rangle = E|\Psi^{\pm}_{\text{eff,out}}\rangle. \tag{60}$$

Ideally, we would require the effective perturbation W_{eff} to vanish faster than the inverse of any interparticle distance as the particles separate to infinity, but if Coulomb tails are present this requirement leads to numerically intractable expressions. Taking our cue from Peterkop [31] and Rudge and Seaton [32,33], we compromise by requiring only that W_{eff} vanishes faster than the inverse of each interparticle distance *as the particles move along classical straight-line asymptotes*. Therefore we express W_{eff} as a linear combination of Coulomb potentials whose effective charges are chosen so that W_{eff} vanishes when the particles follow classical straight-line motion. This is a physically reasonable constraint since three charged particles can reach dynamic equilibrium most efficiently if they shield one another. In the case where one particle is infinitely massive the effective charges satisfy the well-known condition identified by Peterkop [31] and by Rudge and Seaton [32,33].

Thus we replace $|\Psi^{\pm}_{\text{out}}\rangle$ by $|\Psi^{\pm}_{\text{eff,out}}\rangle$ in Eq. (58). The main contribution to the equivalent surface integral comes from the region about a point of stationary phase on the hypersurface [31–33]. Recalling that Q and H_0 commute, Eq. (58) becomes

$$A \approx \langle\Psi^{-}_{\text{eff,out}}|Q(H^{\dagger}-H)G^{+}(E)W_{\text{in}}|\psi_{\text{in}}\rangle \tag{61}$$

$$=\langle\Psi^{-}_{\text{eff,out}}|[(H_0-E)^{\dagger}Q+Q(E-H_0)]G^{+}(E)W_{\text{in}}|\psi_{\text{in}}\rangle \tag{62}$$

$$=\langle\Psi^{-}_{\text{eff,out}}|QW_{\text{in}}|\psi_{\text{in}}\rangle+\langle\Psi^{-}_{\text{eff,out}}|[(W_{\text{eff}}-W_0)Q+QW_0] \times G^{+}(E)W_{\text{in}}|\psi_{\text{in}}\rangle \tag{63}$$

$$=\langle\Psi^{-}_{\text{eff,out}}|QW_{\text{in}}|\psi_{\text{in}}\rangle+\langle\Psi^{-}_{\text{eff,out}}|(W_{\text{eff}}Q+QW_0P-PW_0Q) \times G^{+}(E)W_{\text{in}}|\psi_{\text{in}}\rangle, \tag{64}$$

where in the last step we observed that $QW_0-W_0Q=QW_0P-PW_0Q$. Now we must confront the consequence that results from the failure of our ansatz $|\Psi^{\pm}_{\text{eff,out}}\rangle$ to exactly satisfy the correct asymptotic boundary condition. The effective perturbation W_{eff} vanishes only at the point of stationary phase on the hypersurface, the point at which the particles follow classical straight-line motion, but it is the *neighborhood* of the point of stationary phase, not just the point itself, which provides the dominant contribution to the surface integral. Consequently, the resulting volume integral on the right side of Eq. (64), specifically the term $\langle\Psi^{-}_{\text{eff,out}}|W_{\text{eff}}QG^{+}(E)W_{\text{in}}|\psi_{\text{in}}\rangle$, is formally divergent. However, this is primarily a technical matter; since $|\Psi^{\pm}_{\text{eff,out}}\rangle$ incorporates the essential physics a physically meaningful value of $\langle\Psi^{-}_{\text{eff,out}}|W_{\text{eff}}QG^{+}(E)W_{\text{in}}|\psi_{\text{in}}\rangle$ can be obtained either by spatial averaging [26–28], or by Padé resummation [34] over the basis, as was done for the half-collision problem [20]. Using Eq. (52) to substitute for $G^{+}(E)W_{\text{in}}|\psi_{\text{in}}\rangle$ in Eq. (64), recalling Eqs. (27) and (51), and the adjoint of Eq. (36), and noting that $QW_{\text{in}}|\psi^{+}_{\text{d}}\rangle=Q(W_{\text{in}}-W_{\text{st}})P|\psi^{+}_{\text{d}}\rangle=QW_{\text{d}}|\psi^{+}_{\text{d}}\rangle$, we arrive at the distorted-wave form of the breakup amplitude:

$$A=\langle\Psi^{-}_{\text{eff,out}}|QW_{\text{d}}|\psi^{+}_{\text{d}}\rangle+\langle\Psi^{-}_{\text{eff,out}}|(W_{\text{eff}}Q+QW_0P-PW_0Q) \times G^{+}(E)W_{\text{d}}|\psi^{+}_{\text{d}}\rangle. \tag{65}$$

The second (formally divergent) term on the right side of Eq. (65) compensates for the error in the first term due to the approximate nature of $|\Psi^{-}_{\text{eff,out}}\rangle$. Now we turn to the evaluation of the resolvent.

III. SERIES REPRESENTATION OF THE RESOLVENT

A. Coefficients of the series

In order to sum the series representation of the resolvent efficiently it is necessary to develop some knowledge of the properties of the coefficients $\mathcal{I}_n(2z,w)$. In this subsection we examine the asymptotic behavior of $\mathcal{I}_n(2z,w)$ with respect to large values of the index n. In addition, we establish a recurrence relation for the coefficients, which is stable in the backward direction and can be started from the known value of $\mathcal{I}_n(2z,w)$ at asymptotically large n.

To this end it is useful to change the integration variable in Eq. (16) from s to θ where

$$ws=\tan\theta. \tag{66}$$

The integral over the new variable is

$$\mathcal{I}_n(2z,w)=(-1)^n\int_0^{\theta_w}d\theta\,\sec^2\theta e^{iz\tan\theta-2in\theta}, \tag{67}$$

where the upper limit of integration is

$$\theta_w\equiv\tan^{-1}w. \tag{68}$$

Writing

$$\mathcal{I}_n(2z,w)=\frac{(-1)^n}{iz}\int_0^{\theta_w}d\theta e^{-2in\theta}\left(\frac{d}{d\theta}e^{iz\tan\theta}\right), \tag{69}$$

and repeatedly integrating by parts (by integrating the factor $e^{-2in\theta}$) yields, for $|z|/n\ll 1$,

$$\mathcal{I}_n(2z,w)\sim -i(-1)^n\left(\sum_{m=1}\frac{p_m(z,0)}{n^m}-e^{-2in\theta_w}\sum_{m=1}\frac{p_m(z,\theta_w)}{n^m}\right), \tag{70}$$

where

$$p_m(z,\theta) \equiv \frac{1}{z}\left(\frac{1}{2i}\frac{d}{d\theta}\right)^m e^{iz\tan\theta}. \tag{71}$$

The first sum on the right side of Eq. (70) arises from the lower end point 0 and is independent of w, while the second sum arises from the upper end point θ_w and depends on w.

Since

$$2\cos^2\theta p_1(z,\theta) = z p_0(z,\theta), \tag{72}$$

the $p_m(z,\theta)$ can be evaluated recursively, starting with $p_0(z,\theta)=e^{iz\tan\theta}/z$. Defining

$$q_k(\theta) \equiv 2\left(\frac{1}{2i}\frac{d}{d\theta}\right)^k \cos^2\theta \tag{73}$$

$$= \begin{cases} 2\cos 2\theta, & k=0 \\ \cos 2\theta, & k \text{ even} \geq 2 \\ i\sin 2\theta, & k \text{ odd} \geq 1 \end{cases} \tag{74}$$

and using Leibniz's rule for differentiation gives for $m \geq 0$

$$2\cos^2\theta p_{m+1}(z,\theta) = z p_m(z,\theta) - \sum_{k=0}^{m-1}\binom{m}{k} q_{m-k}(\theta) p_{k+1}(z,\theta). \tag{75}$$

If $\mathrm{Im}(\theta_w)<0$ we have $|e^{-2i\theta_w}|<1$, in which case the prefactor of the second sum (the w-dependent sum) on the right side of Eq. (70) is exponentially small for large n. We can gain insight into the behavior of $p_m(z,0)$ as m increases by approximating $\tan\theta$ by θ in Eq. (71); this shows that $p_m(z,0)$ grows with m as z^m. For $|w| \gg 1$ we have

$$\theta_w \approx \frac{\pi}{2} - \frac{1}{w}, \quad |w| \gg 1 \tag{76}$$

and by approximating $\tan\theta$ by $1/(\frac{\pi}{2}-\theta)$ in Eq. (71) we see that $p_m(z,\theta_w)$ grows with m and w as $(zw^2)^m e^{-\mathrm{Im}(ze^{-i\phi})w}$. Hence we require

$$n \gg |z| \tag{77}$$

for the first sum (the w-independent one) on the right side of Eq. (70) to converge rapidly with m, and we require

$$n \gg |zw^2| \tag{78}$$

for the second sum (the w-dependent one) to converge rapidly with m.

Integration by parts accounts only for the contributions from the end points 0 and θ_w. There is another contribution to the integral $\mathcal{I}_n(2z,w)$, which arises from a saddle point at $\theta=\theta_0$, where

$$\cos^2\theta_0 = z/(2n). \tag{79}$$

The saddle-point contribution is significant provided that the path of steepest descent can be joined to the end points without returning over the ridge. Hence we require that θ_0 lies to the left of θ_w. Assuming that $n \gg |z|$ we have

$$\theta_0 \approx (\pi/2) - \sqrt{(z/2n)}, \tag{80}$$

and recalling Eq. (76) we see that this condition amounts to $n \ll |zw^2|$, the opposite of the condition implied by Eq. (78). Hence, putting $z=Et_\phi$ and $w=\mathcal{T}_{-\phi}$ we find that if

$$n \gtrsim n_{\mathrm{sad}} \equiv (Et_0)\mathcal{T}^2, \tag{81}$$

and if $n \gg Et_0$, the saddle-point contribution to $\mathcal{I}_n(2Et_\phi, \mathcal{T}_{-\phi})$ is negligible, so the end point contributions dominate, while if $n \ll n_{\mathrm{sad}}$ the saddle-point contribution is most important. If z and w are real and positive the saddle point becomes a point of stationary phase [35] and using the method of stationary phase we find that if $|zw^2| \gg n \gg |z|$,

$$\mathcal{I}_n(2z,w) \sim \left(\frac{2\pi^2 n}{z^3}\right)^{1/4} e^{i\sqrt{8zn}+i\pi/4}, \tag{82}$$

a result that may be analytically continued to complex values of z provided that the path of steepest descent can be joined to the end points by paths that cross the "flatlands." If $\mathrm{Im}\sqrt{z}>0$ the saddle-point contribution is exponentially damped for large n by the factor $e^{-\mathrm{Im}\sqrt{8zn}}$. Although the right side of Eq. (82) is explicitly independent of w, it is implicitly dependent on w since it is invalid if $n \gtrsim |zw^2|$.

The integrals $\mathcal{I}_n$, each of which is the sum of the right sides of Eqs. (70) and (82) for large n, can be evaluated efficiently by backward recursion. To derive a recurrence relation we start by using

$$(2 + e^{2i\theta} + e^{-2i\theta}) = 4\cos^2\theta \tag{83}$$

in Eq. (14) to give

$$2\mathcal{I}_n(2z,w) - \mathcal{I}_{n-1}(2z,w) - \mathcal{I}_{n+1}(2z,w) = 4(-1)^n \int_0^{\theta_w} d\theta e^{iz\tan\theta - 2in\theta}. \tag{84}$$

Integrating by parts on the right side of Eq. (84) yields

$$2\mathcal{I}_n(2z,w) - \mathcal{I}_{n-1}(2z,w) - \mathcal{I}_{n+1}(2z,w) = (-1)^{n+1}\left(\frac{2i}{n}\right)(1 - e^{izw-2in\theta_w}) + (-1)^n\left(\frac{2z}{n}\right)\int_0^{\theta_w} d\theta \sec^2\theta e^{iz\tan\theta-2in\theta}. \tag{85}$$

Recognizing that the integral on the right side of Eq. (85) is proportional to $\mathcal{I}_n$ we arrive at the inhomogeneous recursion formula

$$n\mathcal{I}_{n+1}(2z,w) - 2(n-z)\mathcal{I}_n(2z,w) + n\mathcal{I}_{n-1}(2z,w) = 2i(-1)^n(1 - e^{izw-2in\theta_w}), \tag{86}$$

which is valid for $n \geq 0$. In principle we can evaluate $\mathcal{I}_n$ by forward recursion, starting with

$$\mathcal{I}_0(2z,w) = \frac{i}{z}(1 - e^{izw}), \tag{87}$$

$$\mathcal{I}_1(2z,w) = \mathcal{I}_0 + 2i\,\exp(-z)[E_1(-z) - E_1(-z-izw)], \tag{88}$$

where $E_1(z)$ is the exponential integral; but in practice the result is numerically unstable at large n. However, backward recursion is stable. Incidentally, Eq. (87) implies that the correct solution to the recurrence relation is the "regular" one, i.e., the one for which $\mathcal{I}_{-1}(2z,w)$ is finite, since if we put $n=0$ in Eq. (86) and if $\mathcal{I}_{-1}(2z,w)$ is finite we recover Eq. (87).

Returning to the integral representation of $\mathcal{I}_n(2z,w)$, we showed that for large n it can be expressed as the sum of the two end point contributions and a saddle-point contribution. The end point contributions are generated by the inhomogeneous term in the recursion formula. The lower-end point contribution is generated by the w-independent part of the inhomogeneous term, while the upper-end point contribution is generated by the w-dependent part. A particular solution of the inhomogeneous recurrence relation includes the end point contributions, while a solution of the homogeneous recurrence relation includes the saddle-point contribution. Any linear combination of a particular solution and a solution of the homogeneous equation is a solution of the inhomogeneous equation. The correct linear combination can be determined by starting the solution at $n \gg n_{\mathrm{sad}}$ using the asymptotic series for $\mathcal{I}_n(2z,w)$ on the right side of Eq. (70). The w-dependent part of this asymptotic series, i.e., the second series on the right side of Eq. (70), falls off more rapidly with increasing n than a solution of the homogeneous equation, so the correct solution is not contaminated by a solution of the homogeneous equation.

Since the recurrence relation for $\mathcal{I}_n(2z,w)$ depends on w only through the inhomogeneous term the average over w of $\mathcal{I}_n(2z,w)$ can be found directly—it is the solution of the recurrence relation that differs from Eq. (86) only through the replacement of the inhomogeneous term by its w average.

B. Summation of the series

The off-shell contribution to the resolvent is independent of $\mathcal{T}$. This contribution follows from replacing each coefficient $\mathcal{I}_n(2Et_\phi,\mathcal{T}_{-\phi})$ in the series representation on the right side of Eq. (13) by its $\mathcal{T}$-independent part, which for $n=0$ is just (i/Et_ϕ). For $n \gtrsim Et_0$ we can use Eq. (70) to express the $\mathcal{T}$-independent part of $\mathcal{I}_n(2Et_\phi,\mathcal{T}_{-\phi})$ in powers of $1/n$, as $-i(-1)^n\Sigma_{m=1}^{m_0} p_m(Et_\phi,0)/n^m$, where m_0 is a finite positive integer which we leave unspecified except to note that a value of two or three suffices. To obtain a rough estimate, $\mathcal{S}_{\mathrm{off}}(Et_\phi)$ say, of the off-shell contribution to the resolvent we approximate $\mathcal{I}_n(2Et_\phi,\mathcal{T}_{-\phi})$ in powers of $1/n$ for *all* $n \geq 1$; this gives

$$\mathcal{S}_{\mathrm{off}}(Et_\phi) \equiv e^{-t_\phi H}\left[\frac{1}{E} + t_\phi(2t_\phi H)\sum_{m=1}^{m_0} p_m(Et_\phi,0) \times \sum_{n=1}^{\infty}\frac{(-1)^n}{n^{m+1}} L_{n-1}^{(1)}(2t_\phi H)\right], \tag{89}$$

where we have interchanged the order of the sums over m and n. Higher powers of $1/n$ reflect the contributions of higher derivatives with respect to τ of $U(t)$ in the region $\tau \approx 0$. In the high-energy limit the time scale shrinks to zero (i.e., $t_\phi \approx 0$) and we obtain the result $\mathcal{S}_{\mathrm{off}}(Et_\phi) \approx 1/E$. Using Eq. (B17) we can express the infinite sum on the right side of Eq. (89) as a numerically tractable integral; we have

$$\mathcal{S}_{\mathrm{off}}(Et_\phi) = \frac{e^{-t_\phi H}}{E} - t_\phi(2t_\phi H)\sum_{m=1}^{m_0}\frac{p_m(Et_\phi,0)}{m!} \times \int_0^\infty dx e^{-x} x^m \left(\frac{e^{-t_\phi H\tanh(x/2)}}{(1+e^{-x})^2}\right). \tag{90}$$

The integrals over x are well suited to Gauss-Laguerre quadrature.

The remainder of the right side of Eq. (13) contains mostly the on-shell contribution; writing

$$\frac{1 - e^{it_0 E\mathcal{T}}U(t_0\mathcal{T})}{E-H} = \mathcal{S}_{\mathrm{off}}(Et_\phi) + i\mathcal{S}_{\mathrm{on}}(Et_\phi,\mathcal{T}_{-\phi}) \tag{91}$$

and using Eq. (89) we have

$$\mathcal{S}_{\mathrm{on}}(Et_\phi,\mathcal{T}_{-\phi}) \equiv ie^{-t_\phi H}\frac{e^{i(Et_0)\mathcal{T}}}{E} - t_\phi(2t_\phi H) \times \sum_{n=1}^{\infty}\frac{1}{n}\mathcal{J}_n(2Et_\phi,\mathcal{T}_{-\phi})L_{n-1}^{(1)}(2t_\phi H), \tag{92}$$

where $\mathcal{J}_n(2z,w)$ is the modified coefficient

$$\mathcal{J}_n(2z,w) \equiv \mathcal{I}_n(2z,w) + i(-1)^n\sum_{m=1}^{m_0}\frac{p_m(z,0)}{n^m}, \quad n \geq 1. \tag{93}$$

Since we have subtracted the first m_0 terms in powers of $1/n$ the modified coefficient behaves for n in the range $Et_0 \ll n \lesssim n_{\mathrm{sad}}$ as

$$\mathcal{J}_n(2z,w) = \left(\frac{2\pi^2 n}{z^3}\right)^{1/4} e^{i\sqrt{8zn}+i\pi/4} + O\left(\frac{1}{n^{m_0+1}}\right). \tag{94}$$

We assume that n_{sad} is sufficiently large that the term in $1/n^{m_0+1}$ is dwarfed by the saddle-point term over "most" of the range $Et_0 \ll n \lesssim n_{\mathrm{sad}}$. This being the case, we can estimate the on-shell contribution to the resolvent by approximating $\mathcal{J}_n(2z,w)$ by the saddle-point term in Eq. (92). Noting that if $n \gg |z|$ and $\sqrt{8n|z|} \gg 1$,

$$e^{-z}L_n^{(m)}(2z) \approx \frac{1}{(\pi^2 2zn)^{1/4}}\left(\frac{n}{2z}\right)^{m/2}\cos\left[\sqrt{8nz} - \frac{(2m+1)\pi}{4}\right], \tag{95}$$

we have

$$\mathcal{S}_{\mathrm{on}}(Et_\phi,\mathcal{T}_{-\phi}) \approx -\frac{i}{\sqrt{2}}\left(\frac{Ht_\phi^2}{E^3}\right)^{1/4}\sum_n\frac{1}{\sqrt{n}}(e^{i\sqrt{8nt_\phi}(\sqrt{E}-\sqrt{H})} + ie^{i\sqrt{8nt_\phi}(\sqrt{E}+\sqrt{H})}), \tag{96}$$

where the sum is over the range $Et_0 \ll n \sim n_{\mathrm{sad}}$, with the summand independent of $\mathcal{T}$ over this range. Evidently, the largest contribution to this sum comes from those eigenvalues of H

for which the oscillations of $e^{-i\sqrt{8nt_\phi H}}$ are cancelled by the oscillations of $e^{i\sqrt{8nt_\phi E}}$, a condition that expresses energy conservation.

Averaging both sides of Eq. (91) over $\mathcal{T}\sim\mathcal{T}_{\max}$, the left side averages to the resolvent $1/(E-H)$. The value of $\mathcal{T}_{\max}$ depends on the value of the energy spacing ΔE in the neighborhood of E. However, there may be many open (energetically accessible) subchannels and the energy spacing may differ from one partial spectrum (associated with a given open subchannel) to another. Therefore it is convenient to define ΔE to be the *average* energy separation per subchannel. To evaluate ΔE we determine the eigenvalue spectrum of the matrix representation H in the neighborhood of E and we multiply the energy spacing by the number of open subchannels. If E lies above the breakup threshold, we include in this number all continuum subchannels in which one electron has energy less than $E/2$.

The continuous spectrum of H is simulated by a discrete spectrum when H is represented by a finite matrix and that deficiency is exposed after a sufficient number of terms are included in the series representation of the resolvent. Let $|E_1\rangle$ and $|E_2\rangle$ be any two eigenkets of H with adjacent eigenvalues E_1 and E_2 in the neighborhood of E. The separation of these eigenvalues in the series representation of $\mathcal{S}_{\text{on}}$ on the right side of Eq. (92) becomes significant when n is sufficiently large that the outgoing-wave (or ingoing-wave) components of the eigenkets $L_{n-1}^{(1)}(2t_\phi H)|E_1\rangle$ and $L_{n-1}^{(1)}(2t_\phi H)|E_2\rangle$ accumulate phases that differ by more than about π. It is evident from Eq. (95) that if n is large $L_{n-1}^{(1)}(2t_\phi x)$ oscillates rapidly when x varies, as

$$\sin\left(\sqrt{8nt_0x}\cos\frac{\phi}{2}+\frac{\pi}{4}\right).$$

Therefore the discreteness of the pseudocontinuum is exposed when

$$\Delta E\left(\frac{d}{dE}\sqrt{8nt_0E}\right)\cos\frac{\phi}{2}\gtrsim 1, \tag{97}$$

i.e., when $n\gtrsim n_{\max}$ where

$$n_{\max}=\frac{1}{2}\left(\frac{\sec^2(\phi/2)}{Et_0}\right)\left(\frac{E}{\Delta E}\right)^2. \tag{98}$$

Ideally, we require $n_{\max}>n_{\text{sad}}$, which, since typically $\phi\ll 1$, is consistent with $\mathcal{T}<\mathcal{T}_{\max}$.

Finally, we observe that we can evaluate the far-off-shell contribution by using the spectral decomposition. Let $|\mathcal{E}\rangle$ be an eigenket of (the matrix representation of) H which is normalized to unity and has eigenvalue $\mathcal{E}$. The far-off-shell contribution is

$$\sum_{\mathcal{E}>\mathcal{E}_{\max}}\frac{|\mathcal{E}\rangle\langle\mathcal{E}|}{E-\mathcal{E}},$$

with $(\mathcal{E}_{\max}-E)\mathcal{T}_{\max}\gg 1$; eigenvalues larger than $\mathcal{E}_{\max}$ do not contribute significantly to the on-shell part of $G(E)$.

IV. TIME-TRANSLATION OPERATOR

In the previous section we saw that $\mathcal{I}_n(2Et_\phi,\mathcal{T}_{-\phi})$ has a part that decreases exponentially with increasing $n^{1/2}$—this part picks out the on-shell contribution to the series representation of $G(E)$—and a part that falls off only as $1/n$ with increasing n—this part is associated with the off-shell contribution. Despite the slow falloff with increasing n, the off-shell contribution arising from terms $n\gg 1$ is small since consecutive terms in the power series in $1/n$ are of opposite sign resulting in partial cancellation.

This cancellation can be attributed to the failure of the power-series representation of the time-translation operator $U(t)$ to converge to $U(0)=1$ when $u=-1$. Suppose that we truncate the expansion of $U(t)$ after N terms, which gives the trial approximation

$$U_N(t)=e^{-t_\phi H}\left[1-2t_\phi H\sum_{n=1}^{N}\frac{1}{n}L_{n-1}^{(1)}(2t_\phi H)u^n\right]. \tag{99}$$

Not surprisingly, $U_N(0)\neq 1$; we have

$$U_N(0)=e^{-t_\phi H}\left[1-2t_\phi H\sum_{n=1}^{N}\frac{(-1)^n}{n}L_{n-1}^{(1)}(2t_\phi H)\right]. \tag{100}$$

We can re-express the right side of Eq. (100) in a form that displays its deviation from the identity by using

$$e^{-t_\phi H}\sum_{n=1}^{\infty}\frac{(-1)^n}{n}L_{n-1}^{(1)}(2t_\phi H)=-\frac{1}{(2t_\phi H)}(1-e^{-t_\phi H}), \tag{101}$$

a result that follows after some minor rearrangement by putting $u=-1$ and $z=t_\phi H$ in Eq. (8). Writing the sum over N terms in Eq. (100) as the difference of two infinite sums, one starting at $n=1$, the other at $n=N+1$, we obtain

$$U_N(0)=1+(2t_\phi H)e^{-t_\phi H}\sum_{n=N+1}^{\infty}\frac{(-1)^n}{n}L_{n-1}^{(1)}(2t_\phi H). \tag{102}$$

The infinite sum on the right side of Eq. (102) is analyzed in some detail in Appendix B, where it is shown that

$$\sum_{n=N+1}^{\infty}\frac{(-1)^n}{n}L_{n-1}^{(1)}(2t_\phi H)\approx-\frac{(-1)^N}{4N}\{2L_{N+1}^{(1)}(2t_\phi H)+e^{t_\phi H}[N-L_{N+2}^{(0)}(2t_\phi H)]\} \tag{103}$$

for large N. Recalling that H is positive definite, we see from Eq. (95) that if $0<\phi<\pi$ the Laguerre polynomial $L_n^{(1)}(2t_\phi H)$ increases exponentially with increasing $\sqrt{n}$, as

$$e^{\sin(\phi/2)\sqrt{8nHt_0}}.$$

Hence, if $0<\phi<\pi$, the right side of Eq. (103) diverges with increasing N. If $\phi=0$ the right side of Eq. (103) remains finite as N increases, but it oscillates without limit, as $(-1)^N$. However, the *average over large N* of $(-1)^N$ vanishes as $1/N$ with increasing N. It follows that even when $\phi\neq 0$ the large-N average of the right side of Eq. (103) vanishes provided that N does not increase beyond the range where $|\sin(\phi/2)\sqrt{8NHt_0}|\lesssim 1$. Noting that we need not consider eigenvalues of H larger than $\mathcal{E}_{\max}$, we see that the average of $U_N(0)$ is approximately 1 if we average over large N subject to the restriction

$$N\lesssim \frac{1}{8(\mathcal{E}_{\max}t_0)\sin^2(\phi/2)}. \tag{104}$$

Besides improving convergence, averaging over N renders the modification of the coefficients $\mathcal{I}_n(2z,w)$ unnecessary since for large n the difference of $\mathcal{I}_n(2z,w)$ and $\mathcal{J}_n(2z,w)$, on the right side of Eq. (93), vanishes upon averaging. However, in our test calculations we chose to modify the coefficients rather than average over N.

It is useful to evaluate the error $(H-i\frac{d}{dt})U_N(t)$ in the trial approximation $U_N(t)$. To do so we express the time derivative in terms of u as

$$\frac{d}{dt}=\frac{i}{2t_\phi}(1-u)^2\frac{d}{du}. \tag{105}$$

Noting that $L_0^{(1)}(x)=1$ and $L_1^{(1)}(x)=2-x$, we have

$$i\frac{d}{dt}U_N(t)=e^{-t_\phi H}H\sum_{n=1}^{N}L_{n-1}^{(1)}(2t_\phi H)u^{n-1}(1-u)^2 \tag{106}$$

$$=e^{-t_\phi H}H[1-(2t_\phi H)u-L_N^{(1)}(2t_\phi H)u^N + L_{N-1}^{(1)}(2t_\phi H)u^{N+1}]+e^{-t_\phi H}H\sum_{n=2}^{N}[L_n^{(1)}(2t_\phi H) - 2L_{n-1}^{(1)}(2t_\phi H)+L_{n-2}^{(1)}(2t_\phi H)]u^n \tag{107}$$

$$=e^{-t_\phi H}H[1-L_N^{(1)}(2t_\phi H)u^N+L_{N-1}^{(1)}(2t_\phi H)u^{N+1}] - e^{-t_\phi H}H(2t_\phi H)\sum_{n=1}^{N}\frac{1}{n}L_{n-1}^{(1)}(2t_\phi H)u^n \tag{108}$$

$$=HU_N(t)-e^{-t_\phi H}H[L_N^{(1)}(2t_\phi H)u^N - L_{N-1}^{(1)}(2t_\phi H)u^{N+1}]. \tag{109}$$

In the last step but one we used the recurrence relation

$$L_n^{(1)}(2z)-2L_{n-1}^{(1)}(2z)+L_{n-2}^{(1)}(2z)=-2(z/n)L_{n-1}^{(1)}(2z). \tag{110}$$

It follows that

$$\left(H-i\frac{d}{dt}\right)U_N(t)=e^{-t_\phi H}[L_N^{(1)}(2t_\phi H)-L_{N-1}^{(1)}(2t_\phi H)u]u^N. \tag{111}$$

Although $L_n^{(1)}(2t_\phi H)$ increases as $e^{\sin(\phi/2)\sqrt{8nHt_0}}$ with increasing n, the factor u^n decreases more rapidly, as $e^{n\ln u}$, provided that $|u|<1$. Therefore the right side of Eq. (111) vanishes with increasing N for all finite nonzero t. When t is very large $(u\approx 1)$ or very small $(u\approx -1)$ we have $1\mp u\approx \mp 2i(e^{i\phi}/\tau)^{\pm 1}$. At the largest allowed value of τ, which is of order $\mathcal{T}$, we have $\ln u\sim 2ie^{i\phi}/\mathcal{T}$, and therefore the right side of Eq. (111) is small if $N(2/\mathcal{T})\sin\phi$ is large compared to $\sqrt{8N\mathcal{E}_{\max}t_0}$, i.e., if

$$N\gg\left(\frac{\mathcal{E}_{\max}t_0}{2}\right)\left(\mathcal{T}\sec\frac{\phi}{2}\right)^2. \tag{112}$$

When τ is positive but very small $\ln u\sim i\pi-2i\tau/e^{i\phi}$, and therefore the right side of Eq. (111) is small if

$$N\gg(\mathcal{E}_{\max}t_0)/\tau^2. \tag{113}$$

This last inequality cannot be satisfied as τ approaches zero and this is consistent with the fact that $U_N(0)\neq 1$ for finite N. However, since u^N oscillates with N as $(-1)^N$ when $u\approx -1$, the right side of Eq. (111) vanishes when averaged over N, provided that Eq. (104) is satisfied. Hence, aside from observing that we must have

$$\mathcal{T}\gg\sqrt{(\mathcal{E}_{\max}t_0)/N}, \tag{114}$$

we can ignore Eq. (113).

We conclude that the large-N average of $U_N(t)$ approaches $U(t)$ as N increases subject to the constraints imposed by Eqs. (104), (112), and (114). Combining Eqs. (104) and (112) gives

$$\tan\frac{\phi}{2}\ll\frac{1}{2\mathcal{T}(Et_0)} \tag{115}$$

while combining Eqs. (98) and (104) gives

$$\tan\frac{\phi}{2}\gtrsim\frac{1}{2}\left(\sqrt{\frac{E}{\mathcal{E}_{\max}}}\right)\left(\frac{\Delta E}{E}\right). \tag{116}$$

Together, Eqs. (115) and (116) imply that

$$\mathcal{T}\ll\mathcal{T}_{\max}. \tag{117}$$

V. VARIATIONAL PRINCIPLES

In the previous section we derived various inequalities pertaining to the number N of terms in $U_N(t)$. For a given number of terms, we can attempt to improve the accuracy of our approximation to $U(t)$ by employing a variational principle. If $U_{\mathrm{tr}}(t)$ is any trial approximation to $U(t)$ the integral equation

$$U(t)U_{\rm tr}(0) = U_{\rm tr}(t) - i\int_0^t dt' U(t-t')\left(H - i\frac{d}{dt'}\right)U_{\rm tr}(t') \tag{118}$$

may be readily verified by integrating by parts the term in the time derivative, noting that $U(0)=1$ and that H is Hermitian (on a space of square-integrable functions). Since the integrand is of first order in the error in $U_{\rm tr}(t)$, the net error incurred by approximating $U(t-t')$ is of second order.

Let us choose our trial approximation to $U(t)$ to be

$$U_{\rm tr}(t) = U_N^{-1}(0)U_N(t), \tag{119}$$

where $U_N(t)$ was introduced in Eq. (99). A better trial approximation is $\bar{U}_{\rm tr}(t)=\bar{U}_N^{-1}(0)\bar{U}_N(t)$ where the overbar indicates the large-N average. However, it is straightforward to generalize the analysis below to include large-N averaging and for the sake of clarity we work with the simpler trial approximation, Eq. (119). Writing $U(t-t')=U(t)U(-t')$ and using Eq. (111), noting that $U_{\rm tr}(0)=1$, we can rewrite Eq. (118) as

$$U(t) = U_{\rm tr}(t) - iU(t)e^{-t_\phi H}U_N^{-1}(0)\int_0^t dt' U(-t')[L_N^{(1)}(2t_\phi H) - L_{N-1}^{(1)}(2t_\phi H)u']u'^N. \tag{120}$$

Approximating $U(t)$ on the right side of Eq. (120) by $U_{\rm tr}(t)$, writing $U(-t')=e^{iHt'}$, and defining $\tau_{-\phi}\equiv(t/t_0)e^{-i\phi}$, we obtain

$$U(t) \approx \{1 - it_\phi e^{-t_\phi H}U_N^{-1}(0)[\mathcal{I}_N(2Ht_\phi,\tau_{-\phi})L_N^{(1)}(2t_\phi H) - \mathcal{I}_{N+1}(2Ht_\phi,\tau_{-\phi})L_{N-1}^{(1)}(2t_\phi H)]\}U_{\rm tr}(t), \tag{121}$$

with an error that is of second order in the error of $U_{\rm tr}(t)$.

To obtain a variational expression for the resolvent it is expedient to return to Eq. (118). Let us multiply both sides of Eq. (118) by $-it_0e^{i(t_0)E\tau}$ and integrate over $\tau=t/t_0$ from 0 to $\mathcal{T}$. Introducing the trial resolvent

$$G_{\rm tr}(E) \equiv -it_0\int_0^{\mathcal{T}} d\tau e^{i(t_0E)\tau}U_{\rm tr}(t_0\tau) \tag{122}$$

we obtain

$$G(E) = G_{\rm tr}(E) - t_0^2\int_0^{\mathcal{T}} d\tau\int_0^{\tau} d\tau' e^{i(t_0E)\tau}U(t-t')\times\left(H - i\frac{d}{dt'}\right)U_{\rm tr}(t') \tag{123}$$

with it understood that $\mathcal{T}$ is large and is to be averaged over so terms in $e^{i(t_0E)\mathcal{T}}U(\mathcal{T})$ can be discarded. In the first step below we interchange the variables τ and τ', and subsequently reorder the sequence of integration, while in the second step we make the change of variables $\tau'\to\tau'+\tau$:

$$\int_0^{\mathcal{T}} d\tau\int_0^{\tau} d\tau' e^{i(t_0E)\tau}U(t-t')\left(H - i\frac{d}{dt'}\right)U_{\rm tr}(t') = \int_0^{\mathcal{T}} d\tau\int_\tau^{\mathcal{T}} d\tau' e^{i(t_0E)\tau'}U(t'-t)\left(H - i\frac{d}{dt}\right)U_{\rm tr}(t) \tag{124}$$

$$= \int_0^{\mathcal{T}} d\tau e^{i(t_0E)\tau}\int_0^{\mathcal{T}-\tau} d\tau' e^{i(t_0E)\tau'}U(t')\left(H - i\frac{d}{dt}\right)U_{\rm tr}(t). \tag{125}$$

Combining Eqs. (111), (123), and (125) gives

$$G(E) = G_{\rm tr}(E) - t_0^2e^{-t_\phi H}U_N^{-1}(0)\int_0^{\mathcal{T}} d\tau e^{i(t_0E)\tau}\int_0^{\mathcal{T}-\tau} d\tau' e^{i(t_0E)\tau'}U(t')\times[L_N^{(1)}(2t_\phi H) - L_{N-1}^{(1)}(2t_\phi H)u]u^N. \tag{126}$$

Thus we have to evaluate integrals of the form

$$\int_0^{\mathcal{T}} d\tau e^{i(t_0E)\tau}u^n\int_0^{\mathcal{T}-\tau} d\tau' e^{i(t_0E)\tau'}U(t').$$

It can be shown that these integrals satisfy a recurrence relation similar to the one satisfied by the $\mathcal{I}_n$ but with a different inhomogeneous term. We obtain a variational approximation to $G(E)$ by replacing $U(t')$ by $U_{\rm tr}(t)$ on the right side of Eq. (126).

For sufficiently large $\mathcal{T}$ only the range $0\le\tau'\ll\mathcal{T}$ contributes to the integral over τ' on the right side of Eq. (125). If we substitute $\mathcal{T}$ for the upper limit $\mathcal{T}-\tau$ on this integral, the two integrals factorize, and the one over τ' is just $(i/t_0)G(E)$, which becomes $(i/t_0)G_{\rm tr}(E)$ if we replace $U(t')$ by $U_{\rm tr}(t')$. Using this result in Eq. (123) gives

$$G(E) \approx G_{\rm tr}(E) - it_0G_{\rm tr}(E)\int_0^{\mathcal{T}} d\tau e^{i(t_0E)\tau}\left(H - i\frac{d}{dt}\right)U_{\rm tr}(t). \tag{127}$$

Integrating by parts on the right side of Eq. (127), discarding the term in $e^{i(t_0E)\mathcal{T}}U_{\rm tr}(\mathcal{T})$, we arrive at a well-known variational principle [28,36] for the resolvent:

$$G(E) \approx 2G_{\rm tr}(E) - G_{\rm tr}(E)(E-H)G_{\rm tr}(E). \tag{128}$$

VI. TEST APPLICATION

As a test of the formalism developed above, we have applied it to ^1S-wave electron impact ionization of a hydrogen atom initially in its ground state. We assumed the nucleus, whose atomic number is $Z=1$, to be infinitely massive and at rest. We chose the static potential to be the interaction experienced by the incident electron (charge $-e$) when averaged over the ground-state motion of the bound electron. This well-known potential is, with a_0 the Bohr radius,

$$W_{\rm st}(r) = -\frac{Ze^2}{a_0}\left(1+\frac{a_0}{Zr}\right)e^{-2Zr/a_0}, \tag{129}$$

where we excluded the term $-(Z-1)e^2/r$, which vanishes since $Z=1$. If r_{12} denotes the separation of the two electrons, the interaction W_0 is

$$W_0(r_{12}) = \frac{e^2}{r_{12}}, \tag{130}$$

and if $\vec{r}_1$ and $\vec{r}_2$ locate the bound and incident electrons, 1 and 2, respectively, relative to the nucleus, at distances r_1 and r_2, the perturbation in the distorted-wave entrance channel is

$$W_{\rm d}(r_1,r_2,r_{12}) = \frac{e^2}{r_{12}} - \frac{Ze^2}{r_2} + \frac{Ze^2}{a_0}\left(1+\frac{a_0}{Zr_2}\right)e^{-2Zr_2/a_0}. \tag{131}$$

Evidently $W_{\rm d}(r_1,r_2,r_{12})$ is finite at $r_2=0$ (leaving aside the exceptional case when r_1 also vanishes). This is a notable feature because elastic scattering from a Coulomb singularity involves substantial *virtual* energy transfer, which must be built into the description of the ionization process. Consequently, we solve the static-potential-scattering part of the problem exactly, or essentially so, a task that is easy to accomplish using any one of a number of methods; we used the method described in Appendix C, which is highly efficient when a discrete analytic basis is employed.

We represented the ^1S-wave Hamiltonian H of the complete system (electron plus hydrogen atom) on a real discrete basis, symmetrized with respect to the electrons, and composed of the functions

$$S^\kappa_{nl}(r_1)S^\kappa_{n'l}(r_2)Y^{(0,0)}_{l,l}(\hat{r}_1,\hat{r}_2) + 1 \leftrightarrow 2,$$

where $S^\kappa_{nl}(r)$ is the radial Sturmian function

$$S^\kappa_{nl}(r) = \sqrt{(\kappa/n)(n-l)_{2l+1}}(2\kappa r)^{l+1}L^{2l+1}_{n-l-1}(2\kappa r)e^{-\kappa r}, \tag{132}$$

normalized so that $\int_0^\infty dr[S^\kappa_{nl}(r)]^2=1$, and where the angular function $Y^{(0,0)}_{l,l}(\hat{r}_1,\hat{r}_2)$ is the coupling of two spherical harmonics to give an eigenstate of the total angular momentum operator with zero eigenvalue. The inverse length scale of the basis, κ, was chosen to increase with the incident electron momentum; the higher this momentum, the smaller the reaction volume and the larger the "optimum" value of κ. We included values of l in the range $0\le l\le 3$. We limited the ordinal numbers $n-l-1$ and $n'-l-1$ of the radial functions to the range $1\le n'-l\le n-l\le 40$; thus our entire basis consisted of at most 3280 functions of $\vec{r}_1$ and $\vec{r}_2$. Although it is unnecessary to diagonalize the entire matrix representation of the Hamiltonian we did so since a 3280×3280 real symmetric matrix can be diagonalized without great effort. For the static-potential-scattering problem (see Appendix C) we calculated the distortion of the incident plane wave by using a basis composed of the functions $S^\kappa_{n0}(r)$ where, typically, $1\le n\le 70$.

We calculated [37] the inclusive rate for scattering using Eq. (56) together with the variational principle, Eq. (128). In Fig. 3 we show the inclusive cross section (the inclusive rate divided by the incident electron flux) over a range of energies above the breakup threshold. The inclusive cross section decreases smoothly and monotonically with increasing energy but flattens out substantially at higher impact energies and remains of the order of the geometric cross section over the entire energy range considered. We show results obtained using a maximum ordinal number of either 29 or 39 (a total basis size of 1860 or 3280, respectively) and the good agreement between the two sets of results gives confidence in their accuracy.

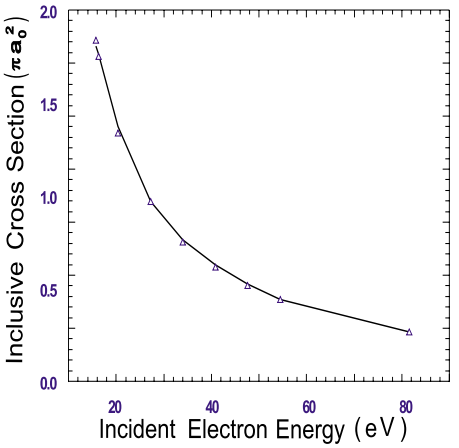

FIG. 3. (Color online) Inclusive cross section for ^1S-wave electron scattering from a hydrogen atom over a range of impact energies above the threshold (13.6 eV) for breakup. Solid curve: present results, basis size 3280. Open triangles: present results, basis size 1860.

In this section we refer to energies relative to the threshold for complete breakup of the system (electron plus hydrogen atom). We take this threshold to be 0 eV, so the lowest possible energy of the system is about −0.527 a.u., corresponding to the only bound state of H^-. Since the Hamiltonian H is represented on a discrete basis all of its eigenvalues are discrete, and with the exception of the lowest eigenvalue, they simulate continuous spectra. Recall that $|\mathcal{E}\rangle$ denotes an eigenket of (the matrix representation of) H, which is normalized to unity and has eigenvalue $\mathcal{E}$. The operator P, which we introduced in Sec. II, projects onto the bound-bound and bound-continuum channels, i.e., onto the entire subspace in which any one electron is in any superposition of hydrogenic bound states. The expectation value $\langle\mathcal{E}|P|\mathcal{E}\rangle$ lies in the interval [0,1] and gives insight into the character of $|\mathcal{E}\rangle$. The closer is $\langle\mathcal{E}|P|\mathcal{E}\rangle$ to unity, the more closely does $|\mathcal{E}\rangle$ describe an eigenstate belonging to either the bound-bound channel, in which both electrons are bound, or the bound-continuum channel, in which one electron remains bound while the other is free. Conversely, the closer is $\langle\mathcal{E}|P|\mathcal{E}\rangle$ to zero, the more closely does $|\mathcal{E}\rangle$ describe an eigenstate belonging to the continuum-continuum channel, in which both electrons are free. In Fig. 4 we show the expectation value of P over a range of energies extending from about −0.527 to 3.0 a.u. Not surprisingly, this expectation value is (very close to) unity at energies below 0 eV, the complete breakup threshold, and it drops abruptly just above

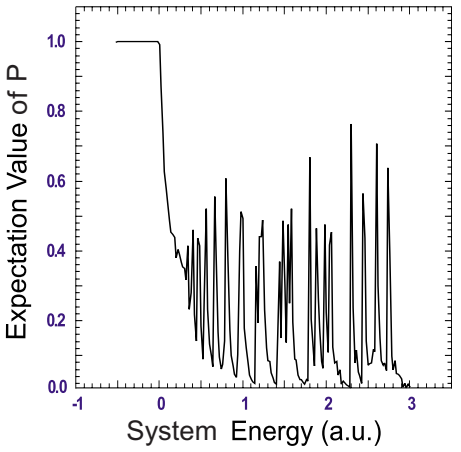

FIG. 4. (Color online) Expectation value of the two-electron projection operator—as in Eq. (133)—which projects onto the ^1S bound-bound- and bound-continuum channels of H^- vs the unshifted eigenvalue spectrum. We smoothed the curve by averaging the expectation value over the tiny energy interval 0.02 atomic units (a.u.). We used a basis with size 3280 and length scale $\kappa=0.7$.

this threshold, where the bound-continuum and continuum-continuum channels are strongly mixed.

The projection operator P can be expressed in terms of projection operators P_1 and P_2, where P_i projects onto the subspace of the full two-electron space in which electron i is bound to the nucleus; we have [38]

$$P = P_1 + P_2 - P_1 P_2. \tag{133}$$

We can write $P_1=(1_1-q_1)\otimes 1_2$, where 1_i is the identity operator for the ith electron and where q_i projects onto the continuum states of the hydrogen atom whose electron is the ith one. Substituting $(1_1-q_1)\otimes 1_2$ and $(1_1-q_1)\otimes 1_2$, respectively, for P_1 and P_2 in Eq. (133) gives

$$P = 1 - q_1 \otimes q_2, \tag{134}$$

where $1=1_1\otimes 1_2$. The complement of P is

$$Q = q_1 \otimes q_2. \tag{135}$$

If $|k_i\rangle$ represents a continuum state of a hydrogen atom whose electron is the ith one we have (with normalization on the momentum scale)

$$q_i = \int_0^\infty dk_i |k_i\rangle\langle k_i|. \tag{136}$$

Note that the product $|k_1\rangle\otimes|k_2\rangle$ does not correctly represent two electrons in the continuum, even at asymptotically large distances, since it does not take into account the long-range electron-electron interaction. Nevertheless, the integral over k_1 and k_2 obtained by combining Eqs. (135) and (136) does correctly describe the projection onto the entire double continuum; this follows from closure. The position-space continuum wave function is (dropping the subscript i for the moment)

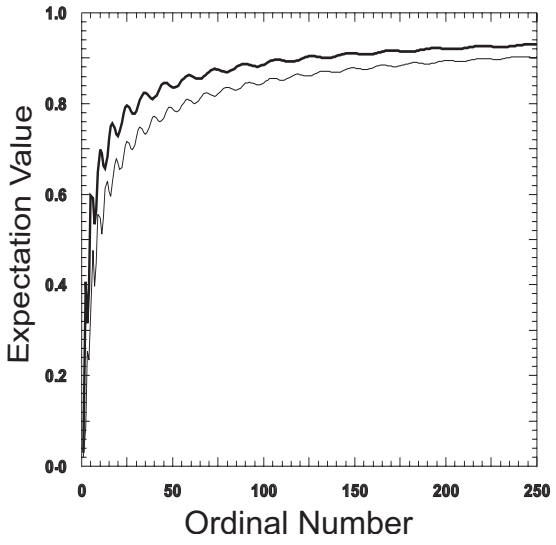

FIG. 5. Expectation value, with respect to the radial basis function $S^\kappa_{n0}(r)$, of the one-electron projection operator—as in Eq. (136)—which projects onto the $l=0$ continuum states of the hydrogen atom vs the ordinal number $n-1$ of the basis, for $\kappa=0.7$ a.u. (thin line) and $\kappa=1.3$ a.u. (thick line).

$$\langle \vec{r}|k\rangle = C_l(2kr)^{l+1}e^{ikr}{}_1F_1(l+1-i\lambda,2l+2;-2ikr)Y_{lm}(\hat{r}), \tag{137}$$

where $Y_{lm}(\hat{r})$ is a spherical harmonic, ${}_1F_1(\ldots)$ is a confluent hypergeometric function, $\lambda=Ze^2/k$, and, up to an irrelevant phase factor,

$$C_l = \sqrt{\frac{2}{\pi}}\frac{|\Gamma(l+1-i\lambda)|e^{(\lambda\pi/2)}}{2\Gamma(2l+2)}. \tag{138}$$

The radial and angular integrals that are involved in the construction of the matrix representations of P and Q can be expressed in closed form. Only the integral over k_i—as in Eq. (136)—needs to be evaluated numerically. It is expedient to change variables from k_i to $x=\tan^{-1}(k_i/\kappa)$, so Eq. (136) becomes

$$q_i = \kappa\int_0^{\pi/2} dx\ \sec^2 x|k_i\rangle\langle k_i|. \tag{139}$$

We performed the integration over x using Simpson's rule.

The radial Sturmian functions overlap both the bound- and continuum-state subspaces spanned by the eigenstates of the hydrogen atom. Since $S^\kappa_{nl}(r)$ is normalized to unity the expectation value $\langle nl\kappa|q|nl\kappa\rangle$ of q $(=q_1$ or $q_2)$ with respect to $S^\kappa_{nl}(r)$ also lies in the interval $[0,1]$ and is a measure of that proportion of a Sturmian function which lies in the continuum. From Fig. 5 we see that as the ordinal number $n-1$ increases the proportion of $S^\kappa_{n0}(r)$ in the continuum increases rapidly, and is about 80% when $n\sim 25$, but this proportion levels off and increases only very slowly as n increases beyond about 40. This indicates that the benefit of increasing the size of a Sturmian basis beyond an ordinal number of roughly 40 is likely to be modest, at least for the description of a scattering process.

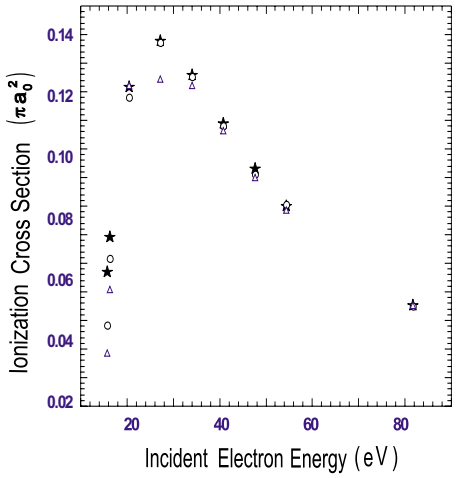

FIG. 6. (Color online) Cross section for ionization of a ground-state hydrogen atom by ^1S-wave electron impact. Stars: data from Bartlett and Stelbovics [9,39]. Open triangles: present results, basis size 1860. Open circles: present results, basis size 3280. The same energy abscissa were used to plot all three sets of data.

In Fig. 6 we show the total cross section for ionization over the same range of energies considered for the inclusive cross section. We calculated the ionization rate by using Eq. (55) together with the variational principle, Eq. (128). Again we show results obtained using a basis size of either 1860 (triangles) or 3280 (circles). The two sets of results agree well at energies above about 40 eV, but the agreement begins to deteriorate as the energy drops below 40 eV. We also show the results (stars) of Bartlett and Stelbovics [9,39], which to our knowledge are the most accurate currently available. At energies above about 25 eV, where the cross section reaches its maximum, the results we obtained with the larger basis agree well with those of Bartlett and Stelbovics, but at energies below where the cross section peaks our results fall too rapidly as the energy drops toward threshold. Our basis is composed of spatially compact functions, which fall off exponentially at large distances, so we would need to include an extremely large number of such basis functions to achieve convergence for energies below about 20 eV, where ionization occurs over a long time interval and the electrons travel far before the process is complete.

Our calculations were performed on a standard desktop with 2 Gb of memory. The execution time was less than 10 min per impact energy. Most of this time was used to completely diagonalize the Hamiltonian matrix; we diagonalized this matrix at each impact energy since the appropriate value of the length scale of the basis (the most important parameter) varies roughly inversely with the impact momentum. The primary source of error lies in the basis.

ACKNOWLEDGMENTS

I am indebted to Bernard Piraux, both for providing me with the matrix elements of $1/r_{12}$ used in the calculations described above and for his collaboration at the initial stage of this work. In addition I thank Philip Bartlett who provided me with tabulated data and kindly carried out additional calculations to supplement the data reported in Ref. [9], thereby affording a more detailed comparison.

APPENDIX A: CHEBYSHEV EXPANSION

Mandelshtam and Taylor [29] derived an expansion of the resolvent in Chebyshev polynomials in the Hamiltonian. They showed that [40]

$$G(E) = -i2t_0 \csc\phi \sum_{n=0}^{\infty} (2-\delta_{n0}) e^{-in\phi} T_n(2Ht_0), \quad \text{(A1)}$$

where $T_n(2Ht_0)$ is a Chebyshev polynomial of degree n. In Eq. (A1) the parameters t_0, ϕ, and the shift Δ in the spectrum of H have definite values, i.e., if $H_{\max}$ and $H_{\min}$, respectively, are the maximum and minimum eigenvalues of the matrix that approximately represents H, we have [40]

$$t_0 = 1/(H_{\max} - H_{\min}), \quad \text{(A2)}$$

$$\phi = \arccos[2(E-H)t_0] - i\gamma, \quad \text{(A3)}$$

$$\Delta = -(H_{\max} + H_{\min})/2, \quad \text{(A4)}$$

where in position space γ is a real positive function of the spatial coordinates which grows with distance. In order to make an appropriate comparison between our approach and the Chebyshev expansion of the resolvent, we put $\mathcal{T} \sim \infty$ in Eq. (13), or, rather, we add a tiny positive imaginary part, η say, to E, so that the left side of Eq. (13) reduces to the resolvent $1/(E-H)$ for $\eta T \gg 1$:

$$G(E) = -it_\phi e^{-t_\phi H} \times \left[I_0(2Et_\phi) - 2t_\phi H \sum_{n=1}^{\infty} \frac{1}{n} I_n(2Et_\phi) L_{n-1}^{(1)}(2t_\phi H) \right], \quad \text{(A5)}$$

where, changing back to the variable $\tau = \mathcal{T}s$ in Eq. (14), letting $\mathcal{T} \to \infty$, and rotating the integration contour through the angle ϕ,

$$I_n(2z) = \int_0^\infty d\tau e^{iz\tau} \left(\frac{\tau + i}{\tau - i} \right)^n. \quad \text{(A6)}$$

A closer comparison can be made after observing that $zL_{n-1}(z)/n$ can be analytically continued to $n=0$ by expressing the Laguerre polynomial as a confluent hypergeometric function in the continuous variable n; we find that $zL_{n-1}(z)/n \to e^z - 1$ as $n \to 0$. Hence we arrive at

$$G(E) = it_\phi (t_\phi H) e^{-t_\phi H} \times \left[\sum_{n=0}^{\infty} \left(2 - \frac{e^{t_\phi H}}{\sinh t_\phi H} \delta_{n0} \right) \frac{1}{n} I_n(2Et_\phi) L_{n-1}^{(1)}(2t_\phi H) \right]. \quad \text{(A7)}$$

Of course, neither Eq. (A5) nor Eq. (A7) are of practical use as they stand because, having taken the limit $\mathcal{T} \to \infty$, the expansions are not convergent due to the branch point at infi-

nite time. However, it is evident that the Chebyshev expansion of the resolvent, Eq. (A1), is the analog of the Laguerre expansion described by Eq. (A7); the Chebyshev expansion emerges from consideration of the spatial behavior of the physical branch, whereas the Laguerre expansion emerges from consideration of the temporal behavior. As shown by Mandelshtam and Taylor [29], the spatial function γ amounts to the inclusion of a complex absorbing optical potential in H. The coefficients $e^{-in\phi}$ in Eq. (A1) contain information about the branch, as do the coefficients $I_n(2Et_\phi)$ in Eq. (A7).

The Chebyshev expansion has been used with considerable success in numerous applications [41]. Its primary disadvantage is that the operator $e^{-\gamma}$ is difficult to evaluate unless γ is diagonalized in position space.

APPENDIX B: EVALUATION OF $\Sigma_n L_n^{(1)}(2z)u^n/n^m$

The sum $\Sigma_{n=0}^N L_n^{(1)}(2z)u^n$ formally converges in the limit $N\to\infty$ for all u inside the unit disk. The infinite sum does not exist at $u=1$ but the limit $N\to\infty$ has a meaning at all other points in the u plane, both on and outside the circumference of the unit disk, as follows from the generating function. The finite sum can be cast in a form suitable for computation by using the contour-integral representation

$$L_n^{(1)}(2z) = \frac{1}{2\pi i}\oint dv e^{-2zv}\left(\frac{1+v}{v}\right)^{n+1}, \tag{B1}$$

where the contour encloses the origin $v=0$ in the counterclockwise sense. Interchanging sum and integral, and evaluating the resulting geometric series, gives

$$\sum_{n=0}^{N} L_n^{(1)}(2z)u^n = \frac{1}{2\pi iu}\oint dv e^{-2zv}\left(\frac{y-y^{N+2}}{1-y}\right), \tag{B2}$$

where

$$y = u(1+v)/v. \tag{B3}$$

In the special case where $u=1$ we have $y/(1-y)=-(1+v)$ and the right side of Eq. (B2) is an integral representation of $L_N^{(2)}(2z)$, so we obtain the well-known result $\Sigma_{n=0}^N L_n^{(1)}(2z) = L_N^{(2)}(2z)$. In general, we cannot evaluate the integral on the right side of Eq. (B2) exactly. To proceed, we expand the contour of integration in order that $|y|<1$ along the entire contour, which is possible as long as $|u|<1$. Thus the contour now encloses both $v=0$ and the point $v=u/(1-u)$ at which $y=1$. Since y^{N+2} vanishes in the limit $N\to\infty$ we have

$$\sum_{n=0}^{\infty} L_n^{(1)}(2z)u^n = \frac{1}{2\pi iu}\oint dv e^{-2zv}\left(\frac{y}{1-y}\right). \tag{B4}$$

The integrand on the right side of Eq. (B4) is nonsingular save for a pole at $y=1$; the integral can be evaluated using Cauchy's residue theorem, which, as expected, yields the generating function on the left side of Eq. (6) for $m=1$. It follows that the finite sum is the difference of the infinite sum and

$$\sum_{n=N+1}^{\infty} L_n^{(1)}(2z)u^n = \frac{1}{2\pi iu}\oint dv e^{-2zv}\left(\frac{y^{N+2}}{1-y}\right) \tag{B5}$$

$$= \frac{1}{2\pi iu(1-u)} e^{-2zu/1-u}\oint dv e^{-2z(v-u/1-u)} \times\left(\frac{vy^{N+2}}{v-\frac{u}{1-u}}\right), \tag{B6}$$

where in the second step we wrote $1/(1-y)=[v/(1-u)]/[v-u/(1-u)]$ and we rearranged the integrand in anticipation of differentiating with respect to z, so as to eliminate the term $v-u/(1-u)$ in the denominator, thereby simplifying the integral. Proceeding accordingly, we have

$$\frac{1}{2\pi i}\frac{d}{dz}\oint dv e^{-2z(v-u/1-u)}\left(\frac{vy^{N+2}}{v-\frac{u}{1-u}}\right)$$

$$= -2\frac{1}{2\pi i}e^{2zu/1-u}\oint dv e^{-2zv} v y^{N+2} \tag{B7}$$

$$= \frac{1}{2\pi i}e^{2zu/1-u}\frac{d}{dz}\oint dv e^{-2zv} y^{N+2} \tag{B8}$$

$$= e^{2zu/1-u}u^{N+2}\frac{d}{dz}L_{N+1}^{(1)}(2z), \tag{B9}$$

where in the last step we used Eq. (B1). The integral on the left side of Eq. (B7) can be evaluated at $z=0$ by expanding the contour of integration to a circle of arbitrarily large radius, along which

$$\frac{vy^{N+2}}{v-\frac{u}{1-u}} \approx u^{N+2} + \frac{u^{N+2}}{v}\left(N+2+\frac{u}{1-u}\right). \tag{B10}$$

The integrand has a pole at $v=0$ and the integral can be immediately evaluated using Cauchy's residue theorem:

$$\frac{1}{2\pi i}\oint dv\left(\frac{vy^{N+2}}{v-\frac{u}{1-u}}\right) = u^{N+2}\left(N+2+\frac{u}{1-u}\right). \tag{B11}$$

Consequently, we arrive at the result

$$\sum_{n=N+1}^{\infty} L_n^{(1)}(2z)u^n = \frac{u^{N+1}}{1-u}e^{-2zu/1-u}\left[N+2+\frac{u}{1-u} + \int_0^z dz' e^{2z'u/1-u}\frac{d}{dz'}L_{N+1}^{(1)}(2z')\right] \tag{B12}$$

$$= \frac{u^{N+1}}{1-u} e^{-2zu/1-u} \left[\frac{u}{1-u} + e^{2zu/1-u} L_{N+1}^{(1)}(2z) - \frac{2u}{1-u} \int_0^z dz' e^{2z'u/1-u} L_{N+1}^{(1)}(2z') \right], \tag{B13}$$

where we integrated by parts and used $L_{N+1}^{(1)}(0)=N+2$.

Assume now that u lies in the neighborhood of -1. Therefore $e^{2z'u/1-u} \approx e^{-z'}$, and since $L_{N+1}^{(2)}(2z')$ oscillates rapidly with z when $N \gg |z|$ the main contribution to the integral over z' comes from the lower end point at $z'=0$. Hence, provided that $N \gg |z|$ we can put $e^{2z'u/1-u} \approx 1$ to give, for the integral over z',

$$\int_0^z dz' L_{N+1}^{(1)}(2z') = \frac{1}{2}[N+2-L_{N+2}^{(0)}(2z)]. \tag{B14}$$

It follows that

$$\sum_{n=N+1}^{\infty} L_n^{(1)}(2z) u^n \approx -\frac{u^N}{4}\{2L_{N+1}^{(1)}(2z) + e^z[N - L_{N+2}^{(0)}(2z)]\},$$

$$u \sim -1. \tag{B15}$$

We know from Eq. (95) that $L_n^{(m)}(2z)$ increases exponentially with increasing $\sqrt{N}$ if z is complex. However, if $|u|<1$ the factor u^N decreases exponentially with increasing N, and hence the right side of Eq. (B15) vanishes in the limit $N \to \infty$ for all z. On the other hand, when $u=-1$ the right side of Eq. (B15) does not vanish as N increases, even if z is real. Integrating both sides of Eq. (B15) over u gives

$$\sum_{n=N}^{\infty} L_{n-1}^{(1)}(2z) \frac{u^n}{n} \approx \frac{u^N}{4N}\{2L_{N+1}^{(1)}(2z) + e^z[N - L_{N+2}^{(0)}(2z)]\},$$

$$u \sim -1. \tag{B16}$$

If $|u|<1$ the right side of Eq. (B16) vanishes in the limit $N \to \infty$ for all z. When $u=-1$ the right side of Eq. (B15) does not vanish as N increases, but if we average over large N, and if z is real, it does vanish since the factor $(-1)^N$ oscillates.

In Sec. III we used the result

$$\sum_{n=1}^{\infty} \frac{e^{-ina}}{n^m} L_{n-1}^{(1)}(z) = \frac{1}{m!} \int_0^{\infty} dx x^m \frac{e^{-x-ia}}{(1-e^{-x-ia})^2} e^{-(e^{-x-ia}/1-e^{-x-ia})z}. \tag{B17}$$

To prove this we use Eq. (B1) together with

$$\frac{1}{n^m} = \frac{1}{m!} \int_0^{\infty} dx x^m e^{-nx}, \tag{B18}$$

to write, for arbitrary a,

$$\sum_{n=1}^{\infty} \frac{e^{-ina}}{n^m} L_{n-1}^{(1)}(z) = \frac{1}{2\pi i m!} \sum_{n=1}^{\infty} \int_0^{\infty} dx x^m e^{-n(x+ia)} \times \oint dv e^{-zv} \left(\frac{1+v}{v} \right)^n \tag{B19}$$

$$= \frac{1}{2\pi i m!} \int_0^{\infty} dx x^m \oint dv e^{-zv} \times \left(\frac{v}{(1-e^{-x-ia})v - e^{-x-ia}} - 1 \right), \tag{B20}$$

where in the second step we interchanged the order of summation and integration and summed the resulting geometric series. Using Cauchy's residue theorem to evaluate the contour integral gives Eq. (B17).

APPENDIX C: POTENTIAL SCATTERING

The s-wave elastic scattering of a particle of mass μ and energy $E_k \equiv k^2/(2\mu)$ from a potential $V(r)$ is governed by the radial Schrödinger equation

$$\left[\frac{1}{2\mu} \frac{d^2}{dr^2} - V(r) + E_k \right] s(r) = 0. \tag{C1}$$

Assuming that $rV(r)$ vanishes for $r \sim \infty$ (i.e., no Coulomb tail),

$$s(r) = \sin kr + \tan \delta (1 - e^{-\beta r}) \cos kr + \zeta(r), \tag{C2}$$

where $\zeta(r)$ is a function of r, which vanishes at $r=0$ and has the same characteristic range as $V(r)$ and where β is a constant whose value can be sensibly chosen to be the inverse of the range of $V(r)$. The prefactor $(1-e^{-\beta r})$ cuts off the irregular free-particle solution $\cos kr$ at $r=0$. The phase shift δ is related to the wave function at the origin through the "cusp condition"

$$\frac{d}{dr} \left(\frac{s(r)}{r} \right) \bigg|_{r=0} = \mu V(r) s(r)|_{r=0}. \tag{C3}$$

If $\mu r V(r)|_{r=0} = C$ the cusp condition becomes

$$\frac{d}{dr} \left(\frac{\zeta(r)}{r} \right) \bigg|_{r=0} = C \left. \frac{\zeta(r)}{r} \right|_{r=0} + Ck + \beta \left(C + \frac{\beta}{2} \right) \tan \delta. \tag{C4}$$

Substituting the right side of Eq. (C2) into Eq. (C1) yields

$$\left[\frac{1}{2\mu} \frac{d^2}{dr^2} - V(r) + E_k \right] \zeta(r) - \left[\left\{ [E_\beta - V(r)] \cos kr + \frac{k\beta}{\mu} \sin kr \right\} e^{-\beta r} + V(r) \cos kr \right] \tan \delta = V(r) \sin kr, \tag{C5}$$

where $E_\beta \equiv \beta^2/(2\mu)$. Equations (C4) and (C5) are a pair of coupled linear equations for $\zeta(r)$ and $\tan \delta$, and they can be

solved readily, and to very high accuracy, by expanding $\zeta(r)$ on a discrete basis [42]. Note that the forward- and backward-evolving distorted wave functions in the entrance channel, which satisfy the boundary condition incorporated in the integral equation, Eq. (49), are $e^{\pm i\delta}\cos\delta s(r)$. If $V(r)$ were to have a Coulomb tail we would have to modify Eq. (C2) by replacing sin kr and cos kr, respectively, by regular and irregular Coulomb wave functions.

[1] T. T. Scholz, H. R. J. Walters, P. G. Burke, and M. P. Scott, J. Phys. B **24**, 2097 (1991).

[2] O. Zatsarinny and K. Bartschat, Phys. Rev. A **77**, 062701 (2008).

[3] C. Bouri, P. Selles, L. Malegat, and M. G. Kwato Njock, Phys. Rev. A **73**, 022724 (2006).

[4] E. J. Heller and H. A. Yamani, Phys. Rev. A **9**, 1209 (1974).

[5] J. Callaway and K. Unnikrishnan, J. Phys. B **26**, L419 (1993).

[6] I. Bray and A. T. Stelbovics, Phys. Rev. A **46**, 6995 (1992).

[7] M. Baertschy, T. N. Rescigno, W. A. Isaacs, X. Li, and C. W. McCurdy, Phys. Rev. A **63**, 022712 (2001).

[8] For a review see C. W. McCurdy, M. Baertschy, and T. N. Rescigno, J. Phys. B **37**, R137 (2004).

[9] P. L. Bartlett and A. T. Stelbovics, Phys. Rev. Lett. **93**, 233201 (2004).

[10] For a tutorial see P. Bartlett, J. Phys. B **39**, R379 (2006).

[11] Z. Papp and C.-Y. Hu, Phys. Rev. A **66**, 052714 (2002).

[12] S. A. Zaytsev, V. A. Knyr, Yu. V. Popov, and A. Lahmam-Bennani, Phys. Rev. A **75**, 022718 (2007).

[13] H. Bachau, E. Cormier, P. Decleva, J. E. Hansen, and F. Martin, Rep. Prog. Phys. **64**, 1815 (2001).

[14] J. S. Parker, B. J. S. Doherty, K. T. Taylor, K. D. Schultz, C. I. Blaga, and L. F. DiMauro, Phys. Rev. Lett. **96**, 133001 (2006).

[15] S. Hu, J. Colgan, and L. Collins, J. Phys. B **38**, L35 (2005).

[16] E. Foumouo, G. L. Kamta, G. Edah, and B. Piraux, Phys. Rev. A **74**, 063409 (2006).

[17] J. Colgan, M. S. Pindzola, G. Childers, and M. A. Khakoo, Phys. Rev. A **73**, 042710 (2006).

[18] L. Nikolopoulos and P. Lambropoulos, J. Phys. B **40**, 1347 (2007).

[19] A. M. Mukhamedzhanov and M. Lieber, Phys. Rev. A **54**, 3078 (1996).

[20] Numerically converged cross sections two-electron escape by one-photon absorption, including energy and angular distributions, were calculated without knowledge of exact asymptotic boundary conditions in M. Pont and R. Shakeshaft, Phys. Rev. A **51**, R2676 (1995); J. Phys. B **28**, L571 (1995).

[21] See also R. Shakeshaft, Phys. Rev. A **76**, 063405 (2007).

[22] The inclusion of a second "hidden" time coordinate has been used to exploit further symmetries. All of the stationary properties of the hydrogen atom, including its hidden symmetry, can be derived in a few lines by considering the hydrogen atom to be the projection of a larger system in a world with two time coordinates; see I. Bars, Phys. Rev. D **58**, 066006 (1998).

[23] R. Shakeshaft and B. Piraux, Adv. Theor. Math. Phys. **4**, 1093 (2000).

[24] If P_{open} projects onto the open subchannels and $P_{\text{closed}}=1-P_{\text{open}}$, we can evaluate the resolvents $1/(E-P_{\text{open}}HP_{\text{open}})$ and $1/(E-P_{\text{closed}}HP_{\text{closed}})$ by rotating the contour and by using the spectral decomposition, respectively.

[25] In earlier work we did integrate up to the branch point and we employed the technique of analytic continuation to deal with the resulting divergence; see T. Li, B. Piraux, and R. Shakeshaft, Phys. Rev. A **67**, 052704 (2003). The technique developed in the present work, based on temporal averaging, is far simpler to implement and affords greater accuracy.

[26] M. Lieber, L. Rosenberg, and L. Spruch, Phys. Rev. D **5**, 1330 (1972).

[27] M. Lieber, L. Rosenberg, and L. Spruch, Phys. Rev. D **5**, 1347 (1972).

[28] L. Rosenberg, Phys. Scr. **77**, 015305 (2008).

[29] V. A. Mandelshtam and H. S. Taylor, J. Chem. Phys. **103**, 2903 (1995).

[30] In case the reader is not familiar with this result, here is a derivation: From $G^{\pm}(E)=G_{\text{d}}^{\pm}(E)+G^{\pm}(E)W_{\text{d}}(E)G_{\text{d}}^{\pm}(E)$ we have $G^{\pm}(E)W_{\text{st}}|\psi_{\text{in}}\rangle=G_{\text{d}}^{\pm}(E)W_{\text{st}}|\psi_{\text{in}}\rangle+G^{\pm}(E)W_{\text{d}}G_{\text{d}}^{\pm}(E)W_{\text{st}}|\psi_{\text{in}}\rangle$, and using these equations together with Eqs. (46) and (49) we obtain $G^{\pm}(E)W_{\text{in}}|\psi_{\text{in}}\rangle=G^{\pm}(E)W_{\text{d}}|\psi_{\text{in}}\rangle+G^{\pm}(E)W_{\text{st}}|\psi_{\text{in}}\rangle=G^{\pm}(E)W_{\text{d}}|\psi_{\text{d}}^{\pm}\rangle+G_{\text{d}}^{\pm}(E)W_{\text{st}}|\psi_{\text{in}}\rangle=G^{\pm}(E)W_{\text{d}}|\psi_{\text{d}}^{\pm}\rangle+|\psi_{\text{d}}^{\pm}\rangle-|\psi_{\text{in}}\rangle$. Equation (50) follows upon recalling Eq. (23).

[31] R. K. Peterkop, Opt. Spektrosk. **13**, 153 (1962).

[32] M. R. H. Rudge and M. J. Seaton, Proc. R. Soc. London, Ser. A **283**, 262 (1965).

[33] M. R. H. Rudge, Rev. Mod. Phys. **40**, 564 (1968).

[34] C. M. Bender and S. A. Orszag, *Advanced Mathematical Methods for Scientists and Engineers* (McGraw-Hill, New York, 1978).

[35] If we change variables from θ to χ where $\theta=\frac{\pi}{2}-\frac{\chi}{\sqrt{n}}$, and write $\tan\theta\approx\frac{\sqrt{n}}{\chi}$, we see that the phase of the integrand is $\sqrt{n}$ multiplied by a smoothly varying function of χ whose derivative vanishes at the point of stationary phase.

[36] E. Gerjuoy, A. R. P. Rau, and L. Spruch, Rev. Mod. Phys. **55**, 725 (1983).

[37] There is more than one way to average over the time $\mathcal{T}$. The averaging can be done implicitly rather than explicitly. Padé extrapolation provides an implicit average, although we did not employ this technique here.

[38] Y. Hahn, T. F. O'Malley, and L. Spruch, Phys. Rev. **128**, 932 (1962); H. Feshbach, Ann. Phys. (N.Y.) **5**, 357 (1958).

[39] The stars at impact energies greater than 16.32 eV represent data not previously published, obtained through private communication with P. Bartlett.

[40] We have rewritten Eq. (3.2) of Ref. [29] to make the analogy with our approach more obvious. In particular, we have observed that the polynomial $Q_n(z,\gamma)$ used in Ref. [29] is a product of two polynomials, each in one variable: $Q_n(z,\gamma)=e^{-n\gamma}T_n(z)$, where $T_n(z)$ is the usual Chebyshev polynomial.

[41] I. Baccarelli, L. Andric, T. P. Grozdanov, and R. McCarrol, J. Chem. Phys. **117**, 3013 (2002).

[42] The linear equations for $\zeta(r)$ and $\tan\delta$ are real. However, since $\tan\delta$ is singular when δ is an odd multiple of $\pi/2$ the solution is unstable for $\delta\approx\pi/2$. In this case we can reformulate the problem using $e^{2i\delta}$ in place of $\tan\delta$; the penalty we pay is that the linear equations for $\zeta(r)$ and $e^{2i\delta}$ are complex.